

https://dspace.org/

Adsorption modelling of desulphurisation of light diesel fuel using chloramine T and polymer supported imidation agent

Kgorane, Nomathemba

2017

https://hdl.handle.net/10539/24856

Kgorane, Nomathemba Annah (2017) Adsorption modelling of desulphurisation of light diesel fuel using chloramine T and polymer supported imidation agent, https://hdl.handle.net/10539/24856

Downloaded from a DSpace repository. https://dspace.org/

Adsorption modelling of desulphurisation of light diesel fuel using Chloramine T and Polymer Supported Imidation Agent

MSc (50/50) RESEARCH PROPOSAL

Prepared by

Nomathemba Kgorane (1307799)

Submitted to

School of Chemical and Metallurgical Engineering, Faculty of Engineering and the Built Environment, University of the Witwatersrand, Johannesburg, South Africa

Supervisor(s): Dr. D. Nkazi

October 2017

DECLARATION

I declare that this dissertation is my own, unaided work, except where otherwise acknowledged. It is being submitted for the degree of Master of Science in Petroleum Engineering in the University of the Witwatersrand, Johannesburg. It has not been submitted before for any degree or examination at any other university.

Signed this _____ day of _____ 20

_____

Nomathemba Annah Kgorane

ABSTRACT

In petroleum industry, sulphur compounds are undesirable due to potential corrosions and environmental challenges associated with these compounds. Sulphur occurs in varies forms in crude oil and petroleum products such as, marcaptans, disulphide, sulphides, disulphide H_2S and thiophenes. Commercial scale refineries utilises hydrodesulphurisation to reduce the sulphur content in fuels, though this technology is associated with high operating and capital cost.

Extractive, adsorptive, oxidative, membrane separation and bio desulphurisation are some of the alternative technology being investigated which have proven not to be as efficient and/or cost effective as compared to hydrodesulphurisation. Adsorption desulphurisation has been effective in separation processes where the sorbate concentrations are low and this technology was used to evaluate the performance of the polymer supported imidation agent (Sodium N-chloro-polystyrene sulphonamide) as an adsorbent in diesel fuel desulphurisation.

A mathematical model simulating adsorption on a fixed was developed. This model incorporates internal mass transfer assuming laminar flow, constant interstitial velocity and an isothermal system. To represent liquid solid equilibrium the Langmuir isotherm was used. The model contains partial differentiate equation that were linearised by using the Euler's forward implicit method, this enabled simulating the model using Microsoft Excel Visual Basic. The obtained simulation results were compared against experimental data. The impact of varying parameters such as initial sulphur concentration, adsorbent bed porosity and external bed surface area per particle volume was studied in detail. Existing isotherms and kinetics were discussed by using experimental data from Fadhel's study.

It was found that the adsorbate residence time is reduced by smaller adsorbent bed porosity resulting in increased adsorption rate. By decreasing the adsorbent particle diameter and an increase in initial sulphur concentration, the breakthrough time is decreased. The experiment data agreed with the simulation results and this validate that the proposed model is applicable to study the performance of fixed bed adsorption processes under isothermal conditions, no axial mixing and constant interstitial velocities.

The results from the analysed Fadhel's data showed that the modelled light oil can be desulphurise to the Euro 5 level requirements, Sulphur <500ppm, by both Chloramine T and Synthesis PI, a complete sulphur removal was achieved using both adsorbents. The desulphurisation rate proved to be faster with Chloramine T as an adsorbent as compared to Synthesis PI. Modelled light oil adsorption obeyed the pseudo-first-order kinetics and the overall adsorption rate was controlled by the chemisorption process.
The diesel fuels study by Fadhel could not be desulphurised to the Euro 5 level. The diesel fuel 1 sulphur concentration was reduced from 12 354 to 11 200ppm and diesel fuel 2 from 1 900 to 800ppm. It was observed that the rate of desulphurisation proved to be faster with diesel fuel 1 as compared to that of diesel fuel 2.

The Freundlich isotherm was found to be a best fit in the adsorption of diesel fuel 1, the attained R square values was 0.881 and 0.435 for Freundlich and Langmuir, respectively. Also the obtained Langmuir separation factor, R_L , of 1 confirmed the that the Langmuir adsorption was unfavourable. This implies that the adsorption rate was controlled by a physisorption process. The diesel fuel 2 desulphurisation process did not fit the studied adsorption isotherms, the attained R square values was 0.433 and 0.218 for Freundlich and Langmuir, respectively. The Langmuir separation factor confirmed in-favourability at 1 and the Freundlich adsorption strength was 6.052, which is very low as compared to that pf diesel fuel 1 at 272.41. Diesel fuel 1 adsorption reaction obeyed the pseudo-second and pseudo-first order kinetics when reacted with Chloramine T and Synthesis PI, respectively. The obtained R squared values were 0.694 and 0.999 for pseudo-second and pseudo-first order, respectively. Diesel fuel 2 obeyed the third order kinetics with both Chloramine T and Synthesis PI, with R squared values calculated at 0.889 and 0.774 for Chloramine T and Synthesis PI reaction, respectively.

DEDICATIONS

This study is dedicated to my family for all the support throughout the study period.

ACKNOWLEDGEMENTS

I wish to acknowledge the School of Chemical and Metallurgical Engineering of the University of the Witwatersrand for providing research facilities for this study. My gratitude also goes to Dr Diakanua Nkazi for guiding and supervising this study without his support I would have not managed to pull this study through.

CONTENTS

DECLARATION i
ABSTRACT ii
DEDICATIONS iv
ACKNOWLEDGEMENTS v
CONTENTS vi
LIST OF FIGURES viii
LIST OF TABLES x
NOMENCLATURE xi
LIST OF ABBREVIATIONS xiii
1. INTRODUCTION 1
1.1 Background 1
1.2 Motivation 2
1.3 Research Aim and Objectives 3
2 LITERATURE REVIEW 4
2.1 Hydro Desulphurisation 5
2.1.1 Process Description 5
2.1.2 Process Chemistry 6
2.1.3 Challenges 6
2.2 Extractive Desulphurisation 7
2.2.1 Process Description 7
2.2.2 Solvent extraction Process 8
2.2.3 Challenges 8
2.3 Membrane Desulphurisation 9
2.3.1 Process Description 9
2.3.2 Challenges 10
2.4 Adsorptive Desulphurisation 10
2.4.1 Process Description 11
2.4.2 Process Chemistry 11
2.4.3 Challenges 12
2.5 Development of adsorption isotherms and kinetics models from first principle 12
2.5.1 Adsorption Isotherms 12

2.5.2 Adsorption Kinetics 17
2.6 Discussion of published adsorption kinetic and isotherm models 19
2.6.1 Desulphurisation adsorption of diesel fuel onto commercially activated carbon 19
2.6.2 The desulphurisation adsorption study of thiophene and benzothiophene onto NiCeY zeolites 28
2.6.3 The desulphurisation adsorption of dibenzothiophene in model diesel fuel on carbonaceous materials loaded with aluminium oxide particles 34
2.7 Mass transfer in adsorption packed bed 39
2.7.1 Mass transfer Zone 39
2.7.2 Stages of Mass transfer 40
2.7.3 External transport 40
2.7.4 Internal transport 41
3 MODELLED EXPERIMENT DATA 43
3.1 Chloramine T and Synthesised PI as adsorbents in model light oil desulphurisation 43
3.2 Chloramine T and Synthesised PI as adsorbents in diesel oil desulphurisation 45
3.2.1 Chloramine T as an adsorbent in diesel oil desulphurisation 45
3.2.2 Synthesised PI as an adsorbent in diesel oil desulphurisation 46
3.3 Investigated optimal operating conditions 47
4 ADSORPTION ISOTHERM AND KINETICS ANALYSIS 50
4.1.1 Analysis Technique 50
4.1.2 Analysis Results 51
5 MODEL DEVELOPMENT FOR MASS TRANSFER IN ADSORPTION PACKED BED 63
5.1 Mathematical Model 63
5.2 Comparison against other models 66
5.3 Simulation Technique 67
5.4 Simulation Parameters 68
5.5 Simulation Results 68
5.6 Simulation model Validation 71
5.6.1 Breakthrough curve 71
6 CONCLUSION 73
7 RECOMMENDATIONS 75
8 BIBLIOGRAPHY 76
9 APPENDICES 79
9.1 APPENDIX A: Langmuir and Freundlich plots for the desulphurization of diesel fuel 2 79
9.2 APPENDIX B: Microsoft Excel Visual Basic Code for Breakthrough Curve 81

LIST OF FIGURES

Figure 1: Sulphur compounds commonly found in crude oil, (Javadli and de Klerk, 2012) 4
Figure 2: Schematic representation of a Hydro desulphurisation unit in a petroleum refinery Laboratories, 2008 5
Figure 3: Schematic representation of an extractive desulphurisation, (Javadli and de Klerk, 2012) 7
Figure 4: LAM A1 batch adsorption process, (Muzic, et al., 2008). 20
Figure 5: Adsorbent capacity versus time (T=50°C, VD = 50 cm3, n = 300min-1 and madsobernt = 2g), (Muzic, et al., 2008)..... 24
Figure 6: Intra-particle diffusion analysis model, (Muzic, et al., 2008). 26
Figure 7: Adsorption isotherms for adsorptive desulfurization of diesel fuel. (Muzic, et al., 2008). ... 26
Figure 8: Effect of adsorption time on the removal of thiophene and benzothiophene over NiCeY zeolite, (Fei, et al., 2017). 31
Figure 9: Effect of adsorption time on the removal of thiophene and benzothiophene over NiCeY zeolite, (Fei, et al., 2017). 31
Figure 10: The effect of temperature on the adsorption of thiophene and benzothiophene over NiCeY zeolite, (Fei, et al., 2017). 34
Figure 11: Mass transfer zone movement demonstration through an activated carbon bed and the resulting breakthrough curve, (Shaverdi, 2012)..... 40
Figure 12: Model light oil sulphur concentration as function of time, using Chloramine T as an adsorbent, Fadhel, 2010 44
Figure 13: Model light oil sulphur concentration as function of time, using Synthesis PI as an adsorbent, (Fadhel, 2010) 44
Figure 14: Diesel fuel 1 sulphur content as function of time, using Chloramine T as an adsorbent, (Fadhel, 2010)..... 46
Figure 15: Diesel fuel 2 sulphur content as function of time, using Chloramine T as an adsorbent, (Fadhel, 2010)..... 46
Figure 16: Diesel fuel 1 sulphur content as function of time, using Synthesis PI as an adsorbent, Fadhel, 2010..... 47
Figure 17: Diesel fuel 2 sulphur content as function of time, using Synthesised PI as an adsorbent, (Fadhel, 2010)..... 47
Figure 18: Desulphurisation efficiency as function of adsorbent dose at t = 40 hrs and C_0 = 1900ppm in Diesel fuel 2, (Fadhel, 2010)..... 48
Figure 19: Residual sulphur content as function of adsorbent dose at t = 40 hrs and C_0 = 1900ppm in Diesel fuel 2, (Fadhel, 2010)..... 48

Figure 20: 1/qe and log qe residual plots respectively 52
Figure 21: 1/qe and log qe line fit plots respectively 52
Figure 22: 1/qe and log qe residual plots respectively 54
Figure 23: 1/qe and log qe line fit plots respectively 54
Figure 24: 1/qe and log qe residual plots respectively 56
Figure 25: 1/qe and log qe line fit plots respectively 56
Figure 26: 1/qe and log qe residual plots respectively 58
Figure 27: 1/qe and log qe line fit plots respectively 58
Figure 28: ln(qe qt) line fit plots respectively 59
Figure 29: Synthesised PI in Model Light Oil ln(Ct) line fit plots 60
Figure 30: Chloramine T in Diesel fuel 1 ln(t/qe) line fit plots 60
Figure 31: Chloramine T in Diesel fuel 2 $1/C_t^2$ line fit plots 61
Figure 32: Synthesised PI in Diesel fuel 1 ln(qe-qt) line fit plots respectively 61
Figure 33: Synthesised PI in Diesel fuel 2 $1/C_t^2$ line fit plots respectively 62
Figure 34: Desulphurisation through adsorption breakthrough curve 69
Figure 35: Bed porosity effect on simulated breakthrough curve 70
Figure 36: External surface area per bed volume effect on simulated breakthrough curve 70
Figure 37: Effect of bed porosity on simulated breakthrough curve 71
Figure 38: Simulation versus Experiment breakthrough curve 72
Figure 39: Simulation versus Experiment breakthrough curve 72
Figure 40: Langmuir and Freundlich plots for Chloramine T as adsorbent of diesel fuel 2 79
Figure 41: Langmuir and Freundlich plots for synthesized PI as adsorbent of diesel fuel 2 80

LIST OF TABLES

Table 1: The activated carbon properties, (Muzic, et al., 2008) 19
Table 2: Commercially activated carbon properties, (Muzic, et al., 2008) 20
Table 3: Extrapolation results and coefficients of the pseudo-first and pseudo-second order adsorption kinetic models and intra-particle diffusion model., (Muzic, et al., 2008) 25
Table 4: Adsorption isotherm constants, correlation coefficients and separation factor, R_L, for the diesel fuel adsorptive desulphurisation, (Muzic, et al., 2008) 27
Table 5: The modelled diesel fuel compositions, (Fei, et al., 2017) 28
Table 6: The Langmuir adsorption isotherm parameters, (Fei, et al., 2017) 32
Table 7: The Freundlich adsorption isotherm parameters, (Fei, et al., 2017) 32
Table 8: The pseudo-first order experimental data fitting at 30, 50 & 70°C, (Fei, et al., 2017) 33
Table 9: The pseudo-second order experimental data fitting at 30, 50 &70°C, (Fei, et al., 2017) 33
Table 10: Langmuir and Freundlich parameters and correlation coefficient for dibenzothiophene on carbonaceous materials, (Nazal, et al., 2015) 37
Table 11: Pseudo-second order kinetic parameters for dibenzothiophene adsorption of the carbonaceous materials impregnated with Al_2O_3, (Nazal, et al., 2015) 38
Table 12: Properties of the diesel fuel, (Fadhel, 2010) 45
Table 13: Desulphurisation efficiency as function of initial sulphur concentration 49
Table 14: Model comparison 66
Table 15: Simulation model parameters 68

NOMENCLATURE

a available surface area of the bed [m^2]

a_p external surface area per unit volume of particle [m^2/m^3]

b Langmuir constant

C energy of adsorption constant [$mg.g^{-1}$]

C_b gas concentration in the bulk flow [mg/m^3 air]

C^* gas phase concentration adjacent to the surface of the particle in equilibrium with the sorbed phase concentration [mg/m^3 air]

C_{in} initial concentration [mg/m^3 air]

C_0 initial concentration [mg/m^3 air]

C_t solute concentration at time t [$mg\ kg^{-1}$]

C_e equilibrium concentration of solute [$mg\ kg^{-1}$]

C_p gas phase concentration within the pores of the particles [mg/m^3 air]

d_p particle diameter [m]

dx length of each section in the bed [m]

D_{ax} axial dispersion coefficient [m^2/s]

D_m molecular diffusion coefficient [m^2/s]

h_m convective mass transfer coefficient [m/s]

K_F Freundlich constant [$kg\ mg^{-1}$]

K_L Langmuir constant [$kg\ mg^{-1}$]

K_2 second rate constant in [$L.mg^{-1}.min^{-1}$]

K_3 third rate constant in [mg^2/L^2min]

k rate constant in [$mg.L^{-1}.min^{-1}$]

k_1 first-order adsorption rate constant [min^{-1}]

k_2 equilibrium rate constant in [g/mg.min]

k_i intra-particle diffusion rate constant in [$mg.g^{-1}.min^{-0.5}$]

k_d desorption constant

k_{ads} adsorption constant

n Freundlich constant related to adsorption intensity

L bed length [m]

N_A mass flux [$mg/m^2.s$]

q mass of adsorbed sulphur per adsorbent surface [$mg\ g^{-1}$]

q_t sulphur adsorption capacity at time [m.mol.g^{-1}]

q_e equilibrium adsorption capacity [mg g^{-1}]

Q_{max} maximum capacity [mg.g^{-1}]

R^2 correlation coefficient

R_L separation factor

t time [min]

q_{max} theoretical maximum adsorption capacity of the adsorbent [mg/g]

q_T total sorbed phase concentration of all the particles [mg/m^3]

Re Reynolds number

Sc Schmidt number

Sh Sherwood number

T temperature [K]

u_s superficial velocity or flow velocity based on empty tube [m/s]

u interstitial velocity in the bed [m/s]

V volume of a solution containing solute [m^3]

v model fuel volume [mL]

W mass of adsorbent [g]

Greek Symbols

ε_b bed porosity

υ kinematic viscosity [m^2/s]

υ_{ads} adsorption rate

υ_d desorption rate

θ adsorbent surface coverage ratio

LIST OF ABBREVIATIONS

AC	Activated Carbon
ACAL5	Activated Carbon loaded with 5% Aluminium Oxide
ACAL10	Activated Carbon loaded with 10% Aluminium Oxide
AL	Aluminium
BDS	Bio-Desulphurisation
CO	Carbon monoxide
CNT	Carbon NanoTubes
CNTAL5	Carbon NanoTubes loaded with 5% Aluminium Oxide
CNTAL10	Carbon NanoTubes loaded with 10% Aluminium Oxide
DBT	Dimethylbenzothiophenes
GO	Graphene Oxide
GOAL5	Graphene Oxide loaded with 5% Aluminium Oxide
GOAL10	Graphene Oxide loaded with 10% Aluminium Oxide
HDS	Hydrodesulphurisation
MOF	Metal Organic Framework
MTZ	Mass Transfer Zone
NMHC	Non-Methane Hydrocarbons
NOx	Nitrogen Oxides
PDE	Partial Differential Equations
PI	Polymer Supported Imidation agent (Sodium N-chloro-polystyrene sulphonamide)
PM	Particulate Matter
THC	Total Hydrocarbon

1. INTRODUCTION

1.1 Background

Petroleum industries are facing a challenge in developing cost effective technologies for producing ultra-low sulphur fuels in order to comply with the increasingly stringent environmental regulations. Sulphur has as negative impact on the environment because during engine combustion it is converted into sulphur oxides which pollutes the environment and affects air quality, (Muzic and Sertic-Bionda, 2013). Sulphur also damage modern vehicles which require high purity fuels. In addition, fuels with high sulphur concentrations decrease the lifespan and effectiveness of catalytic converters, (Muzic and Sertic-Bionda, 2013).

Another important reason for petroleum refineries to remove sulphur from naphtha streams is its nature to poison and deactivate the metal catalysts in units that are subsequently used to enhance the octane rating in the final gasoline blending, (Gary and Handwerk, 1984).

The commercial refineries utilise catalytic hydrodesulphurisation to reduce the sulphur content in fuels. Alternative technologies being investigated such as extractive, adsorptive, oxidative, membrane separation and bio desulphurisation have proven not to be as efficient and/or cost effective as compared to hydrodesulphurisation. However, adsorption is effective in separation processes where the sorbate concentrations are low and can therefore be used in series with Hydrodesulphurisation (HDS) to achieve ultra clean fuels (deep desulphurisation).

Adsorption can be defined as the process whereby a molecule from a gaseous or liquid phase adheres onto a solid surface substrate. Adsorption usually consists of a fixed column packed with a suitable solid adsorbent. A fluid stream with the undesired adsorbates will then flow through the adsorbent for separation. Adsorption is applied in the purification of liquid mixtures like industrial waste effluents. According to Yussuff, et al. (2013) activated carbon was widely used in the waste and water treatment environment however recent observations indicate that it is now applied in large scale separation processes. Yussuff, et al. (2013) further argues that breakthrough curves can be predicted by developing mathematical models that can simulate the adsorption process' behaviour. This is essential during design as detailed fixed bed dynamics analysis and data are required.

Mathematical modelling and prediction of adsorption processes, adsorption equilibrium and breakthrough curves have been studied extensively. Raghavan and Ruthven (1983) made several assumptions to simplify a model of an isothermal adsorption column packed with porous spherical particles. In this study the model was subjected to small step changes in adsorbate concentration. To describe the liquid-solid equilibrium relationship, the assumptions included a linear isotherm. Suresh and Bavu (2010) studied the internal and external mass transfer, laminar flow along the column and varying fluid velocity along the column were considered.

In this research the degree to which the sulphur solutes from a fluid stream were adsorbed using a fixed bed system, through a mathematical model were studied. The impact of varying parameters such as adsorbent particle surface area, adsorbent bed porosity and initial sulphur concentration were studied.

1.2 Motivation

The Commercial refineries utilise catalytic hydrodesulphurisation to reduce the sulphur content in fuels. However, this technology is associated with high capital and operating costs due to, (Irvine, et al., 1999): a) high design pressures and temperatures, b) high catalyst cost with limited catalyst life, c) high utility consumption (especially hydrogen), d) Shortened catalyst life due to deactivation/poisoning of catalyst as result of coking and fouling caused by presence of the sulphur compounds and e) Reduction in the fuel octane rating, as during hydrogenation the olefins are saturated and contribute to octane number enhancement. The refinery operating cost increases as sour crude oils are being processed. Hydrodesulphurisation (HDS) may not be economically viable to achieve the Euro 5 Sulphur requirements.

The acceptable vehicle exhaust emissions are defined by the European emission standards. These emissions comprise of nitrogen oxides (NO_x), total hydrocarbon (THC), non-methane hydrocarbons (NMHC), carbon monoxide (CO) and particulate matter (PM). The Euro 5 PM requirements is <10 ppm, (Babich and Moulijn, 2003).

Since the HDS' capital and operating cost is very intensive, operating HDS in series with an adsorption process can alleviate some of the costs. In this study the adsorption process through a fixed bed is simulated to understand some of the critical parameters that drive the adsorption process. The success of this study will enable an effective and optimum design of the adsorption process. Countries that still need to comply with the more stringent Euro 5 standards will benefit the most.

1.3 Research Aim and Objectives

The aim of this research is to simulate an adsorption process through a fixed bed. To achieve the aim of this study, the following objectives were investigated:

- Develop a mathematical adsorption model for mass transfer in a fixed bed.
- Discussion of the existing isotherms and kinetics models using experimental data.
- Comparative analysis between the proposed and existing models, and validation of the proposed model.

2 LITERATURE REVIEW

Subsequent to carbon and hydrogen, sulphur is present in great quantity in petroleum products. The mass percentage of sulphur in crude oil ranges between 0.03 to 7.89%, (Mehran, et al., 2007). Sulphur in naphtha streams is removed to avoid sulphur oxides (SO_X) production, which are produced during engine combustion of locomotives, aircraft, automotive vehicles, etc., (Ramraj and Anandaraj, 2014). In addition, fuels with high sulphur concentrations decrease the lifespan and effectiveness of catalytic converters (emission gas treatment systems) in vehicles, (Muzic and Sertic-Bionda, 2013).

Octane rating is essential in the combustion of petrol engines as it reduces uncontrolled ignition that result in engine knocking, and during desulphurisation the octane rating in reduced. Thus desulphurisation technologies are aimed at reducing the sulphur content whilst minimising octane rating losses. It is also essential that the operating cost in optimised by achieving a high desired liquid yield.

According to Agarwal and Sharma (2010) sulphur compounds exist in two forms inorganic and organic, inorganic sulphur such as elemental sulphur, pyrite and hydrogen sulphide (H_2S) can be in a dissolved or suspended form. Javadli and de Klerk (2012), further states that the main sources of sulphur compound in crude oil rich in heavy distillate (i.e. high viscosities and densities) are organic, namely thiophenic, sulphides and thiols and some of the important classes of organic sulphur compounds are indicated in Figure 1.

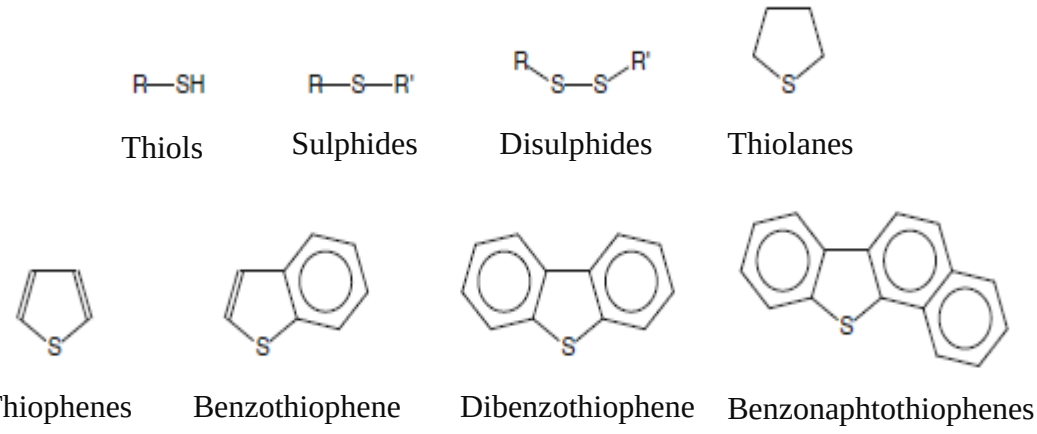


Figure 1: Sulphur compounds commonly found in crude oil, (Javadli and de Klerk, 2012)

Several processes have been proposed in the past or are being used commercially to deal with the problem of removing these compounds from light oil.

2.1 Hydro Desulphurisation

Hydrodesulphurisation (HDS) is a catalytic chemical reaction used to eliminate sulphur compounds from natural gas and refined petroleum products such as gasoline/petrol, diesel, jet fuel and fuel oils, (Ramraj and Anandaraj, 2014). The fuel in which sulphur should be removed from is reacted with hydrogen in a presence of a catalyst to produce H_2S. H_2S is further processed for recovery of solid sulphur and the resulting fuel meet environmental standards, and is processed to final valuable products, (Ramraj and Anandaraj, 2014). An HDS unit is also referred to as a hydro-treater in the petroleum refining industry.

2.1.1 Process Description

Fixed-bed reactors are commercially used for HDS reactions with operating temperatures &pressures ranging from 300 - 400 °C and 30 - 130 atm, respectively, (Gary and Handwerk, 1984). The reactor is packed with an alumina base catalyst which is impregnated with cobalt and molybdenum (Co-Mo). Figure 2 shows a representation of a refinery HDS unit.

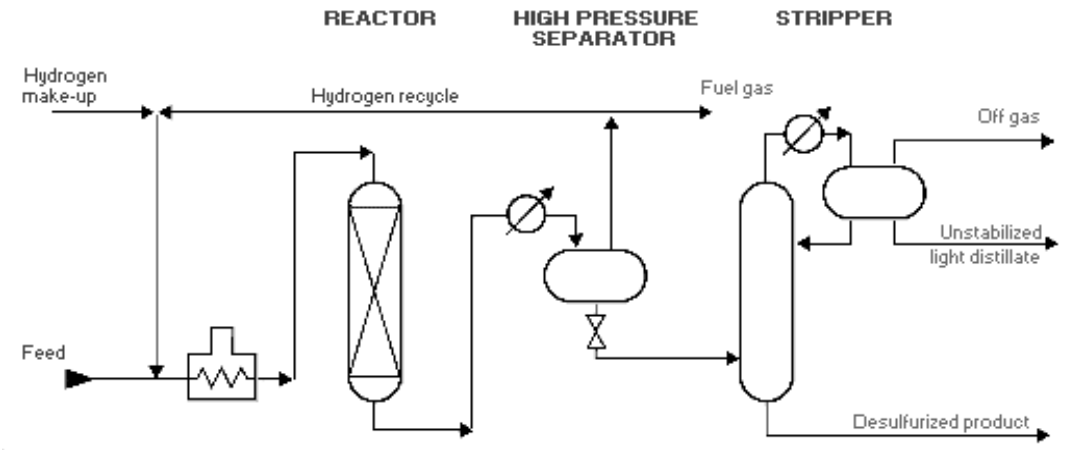


Figure 2: Schematic representation of a Hydro desulphurisation unit in a petroleum refinery Laboratories, 2008

Sulphur compounds in the hydrocarbon feedstock are reacted with hydrogen to produce H_2S, (Gary and Handwerk, 1984). The reactor effluent is cooled to low temperatures and thereafter fed into a liquid/gas separator. Hydrogen rich gas is recovered in the gas separator and recycled back to the reaction stage and the H_2S is sent to a gas treating unit where H_2S is removed. The resulting fuel is thereafter further processed.

2.1.2 Process Chemistry

Hydro desulphurisation is a hydrogenolysis reaction in which a C-X chemical bond is formed, where C is a carbon atom and X can be a sulphur (S), nitrogen (N_2) or oxygen (O_2) atom, (Gary and Handwerk, 1984). Hydrogenolysis reaction results in C-H and H-X chemical bonds whereas hydrogenation is a chemical reactions resulting is the addition of hydrogen (H_2), (Gary and Handwerk, 1984). As an example a hydro desulphurisation of Ethanethiol (C_2H_5SH) can be expressed as follows:

$$C_2H_5SH + H_2 \rightarrow C_2H_6 + H_2S$$

2.1.3 Challenges

This technology has the following challenges:

- High capital and operating cost due to high design temperature and pressure, high operating temperature and pressure, high catalyst cost with limited catalyst life and high hydrogen consumption.
- The refining operating cost increases as crude oils rich in heavy distillate (i.e. sour crudes) are being processed, as a result of the following reasons, (Javadli and de Klerk, 2012):
    - High sulphur content results in catalyst deactivation/poisoning as a result of coking and fouling.
    - Thiophenic sulphur compounds are protected and this makes adsorption for HDS difficult.
- This process reduces the octane rating as during hydrogenation olefins which have a high octane rating are saturated.

- It is not effective in removing refractory organosulphur compounds.

Hence recent research focuses on improving HDS catalysts lifespan and selectivity, and developing alternative cost effect technologies.

2.2 Extractive Desulphurisation

This desulphurisation technology involves a liquid-liquid extraction process. It is highly dependent on the solubility of the sulphur compounds in the solvent of choice and it is critical that the liquid phases are immiscible.

2.2.1 Process Description

According to Babich & Moulijn (2003) and Javadli & de Klerk (2012) the extractive desulphurisation process is as follows: In a mixing tank a solvent and a hydrocarbon liquid with high sulphur content are mixed. During the mixing sulphur compounds that are highly soluble in the solvent of choice are extracted from the hydrocarbon liquid and thereafter the solvent and hydrocarbon liquid are separated. The desulphurised hydrocarbon liquid can be process further and the sulphur compounds in the solvent are removed through distillation. The recovered solvent is recycled back into the mixing tank. Extractive desulphurisation is an attractive method because of it straight forward industrial application. There is no Hydrogen requirement and process operating conditions are moderate, the mixing phase can be operated at near-ambient conditions. Refer to Figure 3 for a schematic representation.

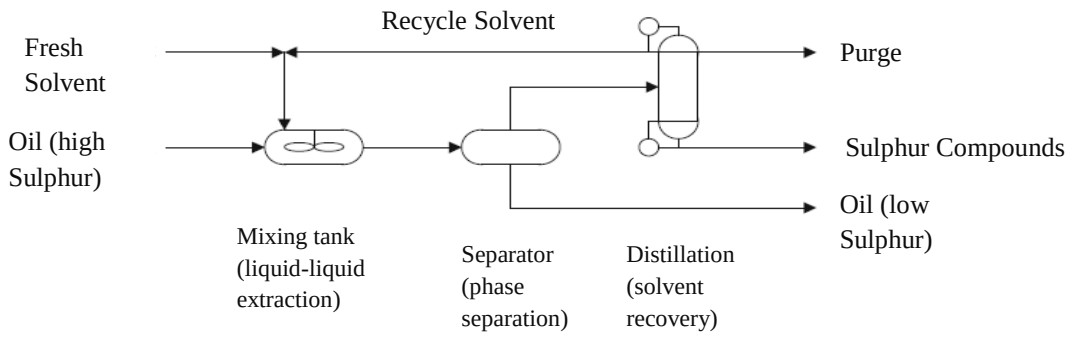


Figure 3: Schematic representation of an extractive desulphurisation, (Javadli and de Klerk, 2012)

2.2.2 Solvent extraction Process

Solvent selection is very critical in this process because the adsorption efficiency is limited by the solubility of the organosulphur compounds in the solvent, (Javadli & de Klerk, 2012). Increasing the polarity of the organosulphur compounds, by oxidising the compounds to sulphones, can potentially improve solubility. Also solubility can be improved by mixing solvents, (Javadli and de Klerk, 2012).

2.2.3 Challenges

According to Javadli and de Klerk (2012) extractive desulphurisation has the following challenges:

- The efficiency is limited by the ability of the organosulphur compounds to dissolve in the solvent, thus for an efficient desulphurisation solvent selection is very critical.
- To ensure effective separation between the solvent and oil, the two phases must be immiscible. To limit the loss of the solvent, the solvent should have low equilibrium solubility in the oil.
- To improve mixing and extraction, the oil and solvent viscosity should be low. This becomes a problem for heavy oil as they have high viscosities; to reduce the viscosity, the extraction has to be performed at high temperatures. The extraction may also have to be conducted under pressure to prevent solvent volatility limitation.
- The volume of the solvent is required to be high relative to that of the extracted sulphur compounds hence the use of higher boiling point solvents is preferred. Higher boiling point solvents are not an option for heavy oil and the use of lighter boiling solvent increases the solvent recovery cost significantly.
- The sulphur compound recovered in the solvent cannot be removed efficiently during distillation and this result in solvent losses.

2.3 Membrane Desulphurisation

This technology involves selective transportation of material through a membrane (permeate), (Hamad, et al., 2011). The material that is not transferred remains in the feed side of the membrane which is referred to as a retentate. There are different driving forces for permeated components; it can either be pressure or concentration, (Hamad, et al., 2011). Processes that depend on pressure driving forces are known as pervaporation processes and membrane processes that depend on concentration gradients across the membrane are known as perstraction processes.

2.3.1 Process Description

Pressure driven membrane desulphurisation, (Hamad, et al., 2011)**:** A sulfur rich hydrocarbon liquid is introduced on the retentate side of a porous membrane and the solvent on the permeate side of the porous membrane. To allow the solvent to extract sulfur compounds from the hydrocarbon liquid, the membrane provides a controlled interface. The proposed membrane contactor relies on extractive liquids to solubilize and transfer the sulfur compounds through the pores of the membrane, so that the transfer rate of the sulfur compounds is not hindered. The membrane contactor brings the extractive liquid and the liquid feed stream into controlled contact without intermixing. The requirements for creating a vacuum or to convert the permeate in a gaseous phase in order to enhance the transport of the sulfur compounds are prevented, and the operating costs associated with the use of vacuum and energy of vaporisation are eliminated.

Concentration driven membrane desulphurisation, (Hamad, et al., 2011)***:*** A concentration driven extraction is a process by which molecules move from high concentrated into a less concentrated solution.

The function of a membrane is to act as a contactor. It will allow the two liquid phases (unrefined liquid hydrocarbons and extractive liquid) to be in direct contact with each other without dispersing one phase into the other. The membrane contactors are used in this extraction process because of the following benefits:

- The membrane brings the extractive liquid and the unrefined liquid hydrocarbon stream into controlled contact without intermixing. This also prevents the unrefined hydrocarbon stream from flooding the extractive liquid side.
- It provided a high contactor surface area between the two phases per unit extractor volume that maximises the molecule transfer rate.

2.3.2 Challenges

The following challenges were highlighted in (Hamad, et al., 2011):

- In pressure driven membrane desulphurisation, the permeate transport rate is increased by changing material into gaseous phase. The material is transformed by heating and/or vacuum and this increases the energy requirements.
- In dense polymeric membrane layers transport agents are required to improve the transport rate of sulphur compounds. Transport agents generally cause plasticising of the selective membrane and has a damaging impact on its selectively to sulphur compounds.
- Dispersed phase contactors are an alternative in reducing sulphur content in hydrocarbons. However these contactors require high solvent holdup which results in emulsion formation, flooding, foaming and unloading. Furthermore liquid-liquid extraction is a conventional technique in which two liquids are intermixed. Slow phase separation and stable emulsions production are draw backs, resulting in the need to produce high surface area for mass transfer.

2.4 Adsorptive Desulphurisation

In this technology organic sulphur compounds are adsorbed onto a solid adsorbent, the process can either be chemical or physical. Thus the efficiency of this method depends on the adsorbent material properties and selectivity to the organic sulphur compounds. The interaction between the sulphur compounds and the adsorption sites should be selective. If the interaction is too strong it will results in desulphurisation and too weak interaction may results in low adsorption selectivity and low capacity, (Sakanishi, et al., 2003).

Even though it is not as effective as HDS, adsorption has the following favourable advantages, (Fadhel, 2010):

- It has a potential of removing refractory sulphur compounds as it is effective in removing low sorbate concentrations.
- It is associated with low operating costs as compared to other desulphurisation processes as it can occur at low temperatures and pressures and the adsorbents can be regenerated
- The sorbent properties are a function of their structure and composition, by altering sorbent structures and composition there can be a potential of optimizing the sorbent properties to maximise the desulphurisation capacity and sulphur selectivity.

2.4.1 Process Description

The adsorptive desulphurisation process can either be chemical or physical as follows:

- Physical adsorption – in this process sulphur compounds are not chemically extracted and according to Javadli and de Klerk (2012) the required regeneration energy is dependent on the strength of the adsorption and is not as high as compared to that of HDS.
- Reactive adsorption – this process entails a chemical reaction between the solid sorbent surface and the sulphur compounds, (Javadli and de Klerk, 2012).

2.4.2 Process Chemistry

This is only applicable to reactive adsorption. Similar to HDS the sulphur compound is attached onto the solid sorbent surface as sulphide. Depending on the nature of the feedstock the adsorbent sulphur is recovered as H_2S or SO_x through flushing spent sorbent with de-sorbent or through thermal sorbent regeneration, (Babich and Moulijn, 2003).

2.4.3 Challenges

To understand the efficiency of varies sorbent, Salem (1994) and Salem (1997) evaluated different desulphurisation sorbent materials under mild reaction plant piloting conditions. Sorbents such as zeolites, activated carbon and metal organic framework (MOF) sorbents amorphous silica-aluminas were used. These sorbents can be used in the desulphurisation of various refinery hydrocarbon liquids, (Javadli and de Klerk, 2012). Salem (1994) and Salem (1997) found that even though the degree of desulphurisation was acceptable, the most efficient of the adsorbents' performance was insufficient for industrial applications, (Javadli and de Klerk, 2012). The narrow pores of large heavy oil molecules' make the accessibility for adsorptive desulphurisation a challenge, (Javadli and de Klerk, 2012). Many of the problems encountered during catalytic HDS are mirrored by adsorptive desulphurisation because both methods depend on adsorption on a solid surface.

2.5 Development of adsorption isotherms and kinetics models from first principle

2.5.1 Adsorption Isotherms

Adsorption is described through isotherms, (Darwish, 2015). These isotherms demonstrate the correlation between the amount of adsorbate on an adsorbent as a function of its pressure (if gas) or concentration (if liquid) at constant temperature. In an adsorption process, adsorbates are adsorbed onto the surface of an adsorbent:

$$\text{Adsorbate} + \text{Adsorbent} \leftrightarrow \text{Adsorption}$$

$$A + B \leftrightarrow AB$$

According to Castellan (1983) the adsorption of solids onto a surface can be classified into two categories, physisorption and chemisorption. In physisorption the adsorbate is bonded onto the solid through the van der Waals interaction (Van der Waals interactions are weak attractions that occur between molecules in close proximity to each other). In this type of

adsorption a multi-layered reaction is possible but the process can be easily disrupted by an increase in temperature. In Chemisorption only a monolayer adsorption is feasible as this process involves a more specific binding of the adsorbate onto the solid.

The difference between the physical and chemisorption can be illustrated by the behaviour of nitrogen adsorption onto iron molecules. At the temperatures of -190°C (temperatures of liquid nitrogen), nitrogen molecules are physically adsorbed onto iron of liquid nitrogen, (Castellan, 1983). However, as the temperature increases the amount of N_2 molecules adsorbed decreases. At room temperature N_2 cannot be adsorbed onto iron. Nitrogen chemisorption is only feasible at temperatures higher than 500°C and it is adsorbed as nitrogen atoms, (Castellan, 1983).

According to Castellan (1983) the adsorption process depends on the following factors:

- ***Temperature***: Due to forces of attraction that exists between an adsorbate and an adsorbent heat energy is released during adsorption thus this process is exothermic, thus adsorption increases at low temperatures. According to Le Chatelier principle, low temperature conditions will favour the forward direction.

  $$\text{Adsorbate} + \text{Adsorbent} \leftrightarrow \text{Adsorption} + \text{energy}$$

- ***Pressure:*** There is a limited number of vacancies on the adsorbent surface thus when all the adsorbent sites are occupied a further increase in pressure will not make any difference in the adsorption process, once saturation pressure is reached adsorption does not occur anymore (i.e. Adsorption is independent of pressure at high pressures).

- ***Surface Area***: Adsorption is surface dependent hence it will increase with an increase in surface area.

- ***Activation of Adsorbent***: To provide more vacant sites on the adsorbent's surface, the adsorbent has to be activated. The activation can be achieved by breaking the adsorbent crystal to expose more sites and also heating adsorbent at higher temperatures.

Two of the most eminent adsorption isotherms that will be analysed in this study are Langmuir and Freundlich.

2.5.1.1 Langmuir Isotherms

The Langmuir Isotherms best describe the chemisorption process. Langmuir's isotherm requires the following assumptions, (Castellan, 1983):

- The adsorbent surface is in contact with an adsorbate solution which is strongly attracted to the surface.
- The adsorbent surface has available sites for solute molecules to be adsorbed.
- The adsorption is monolayer (i.e. only one layer of molecule can be attached to the adsorbent surface).

According to Masel, 1996, the Langmuir equation can be kinetically derived as follows: A monolayer adsorption chemical reaction can be represented by:

$$A + S \leftrightarrow AS$$

AS represents a solute molecule bonded onto an adsorbent surface S. The equilibrium constant K_{ads} for this reaction is given by:

$$K_{ads} = \frac{[AS]}{[A][S]} \quad (2\text{-}1)$$

Where [A], [S] are concentrations of A and S respectively. The [AS] is a two-dimensional concentration. The chemical equilibrium principle is applicable. Equation 2-1 is considered in terms of surface coverage which is defined as the fraction of the adsorption sites to which a solute molecule has become attached. An expression for the fraction of the surface with unattached sites can be expressed as 1 - θ. Given these definitions, we can rewrite the term $\frac{AS}{S}$ as:

$$\frac{[AS]}{S} = \frac{\theta}{1-\theta} \quad (2\text{-}2)$$

Now we express [A] as C and rewrite eqn. 1 as:

$$K_{ads} = \frac{\theta}{C(1-\theta)} \quad (2\text{-}3)$$

The final form of Langmuir adsorption isotherm can be expressed as follows:

$$\theta = \frac{K_{ads}C}{1+K_{ads}C} \quad (2\text{-}4)$$

If Y is defined as the adsorbate amount per adsorbent mass, and Y_{max} is the maximal adsorption, then:

$$\theta = \frac{Y}{Y_{max}} \quad (2\text{-}5)$$

Let $Y = q$ and $K_{ads} = K_L$. At equilibrium the isotherm can be expressed as, Darwish, 2015:

$$q_e = q_{max}\frac{C_e K_L}{1+C_e K_L} \quad (2\text{-}6)$$

The linear form of equation of (2-6) can be expressed as, (Darwish, 2015):

$$\frac{1}{q_e} = \frac{1}{q_{max}K_L}\frac{1}{C_e} + \frac{1}{q_{max}} \quad (2\text{-}7)$$

Where q_{max} is the theoretical maximum adsorption capacity of the adsorbent (mg/g) and K_L indicates a binding constant which is related to the heat of adsorption. All the constants are specific to experiment conditions and the adsorbent type. The plots of $\frac{1}{q_e}$ versus $\frac{1}{C_e}$ and Log q_e versus Log C_e can be used to test the Langmuir and Freundlich adsorption models respectively. To determine the adsorption progression, the separation factor R_L will be calculated. This factor is expressed as, (Lam and Ridzuan, 2008):

$$R_L = \frac{1}{1+K_L C_0} \quad (2\text{-}8)$$

Where K_L was derived from the Langmuir isotherm and C_0 being the sulphur initial concentration on the diesel fuel. The R_L value indicates the shape of the isotherm to be irreversible *(R_L=0)*, favourable *(0< R_L<1)*, linear *(R_L=1)* or unfavourable *(R_L>1), (*Lam & Ridzuan, 2008).

2.5.1.2 Freundlich Isotherms

This isotherm describes an empirical correlation between the solute concentrations on the surface of an adsorbent, to the concentration of the solute in the liquid with which it is in contact with.

Freundlich Adsorption equation can be expressed as:

$$\frac{x}{m} = KP^{\frac{1}{n}} \tag{2-9}$$

Where *x* is the adsorbate mass, *m* is adsorbent mass, *P* is reaction pressure and *K*, *n* are constants depending on reaction temperature. Adsorption is directly proportional to pressure at low pressures ($\frac{x}{m} \propto P^1$) and at high pressures, it is independent of pressure ($\frac{x}{m} \propto P^0$). It was determined experimentally that the Freundlich adsorption isotherms are pressure dependent until saturation is reached. Beyond saturation the rate of adsorption remain the same.

Using a constant of proportionality k in the mass pressure relationship above, equation (2-8) is obtained $\frac{x}{m} = KP^{\frac{1}{n}}$

The linear form of Freundlich's adsorption equation can be expressed as:

$$\log\left(\frac{x}{m}\right) = logK + \frac{1}{n}logP \tag{2-10}$$

Equation (2-10) can also be represented as, (Darwish, 2015):

$$\log(q_e) = logK + \frac{1}{n}logC_e \tag{2-11}$$

Where q_e is the equilibrium adsorbate per gram of the adsorbent, C_e is the equilibrium adsorbate concentration, K_F and *n* are constants. K_F is measure of adsorptive capacity (it is a function of adsorption energy and temperature), and *1/n* determines adsorption strength. This isotherm does not provide information on the monolayer adsorption capacity, Langmuir model does.

2.5.2 Adsorption Kinetics

The adsorption process design is dependent on the process kinetics thus predicting the adsorption rate is critical to the system's design (i.e. adsorbate residence time and the reactor dimensions are dependent on the system's kinetics, (Ho, 2006). Process kinetics is also used in the following:

- Determining the impact of other process parameters (e.g. initial sulphur concentration) on the reaction rate.
- Determining time taking to reach equilibrium, (Mittal, et al., 2006)
- In understanding the adsorption process dynamics with regards to order of rate constant.

The Zero-Order, First-Order, Second-Order and Third-Order are represented by the equations below:

Zero-Order, (Thajeel, 2013):

$$C_t = C_i - k_t \tag{2-12}$$

Where: k is the rate constant in ($mg.L^{-1}.min^{-1}$). C_i and C_t are concentrations at time t, respectively (mg/L).

First-Order, (Thajeel, 2013):

$$ln\, C = ln\, C_i - K_t \tag{2-13}$$

Where: K is the first rate constant in (min^{-1}). C_i and C_t are concentrations at time t, respectively (mg/L).

Second-Order, (Thajeel, 2013):

$$\frac{1}{C_t} = \frac{1}{C_i} + K_2 t \tag{2-14}$$

Where: K_2 is the second rate constant in (L.mg^{-1}.min^{-1}). C_i and C_t are concentrations at time t, respectively (mg/L).

Third-Order, (Thajeel, 2013):

$$\frac{1}{C_t^2} = \frac{1}{C_i^2} + K_3 t \quad (2\text{-}15)$$

Where: K_3 is the third rate constant in (mg^2/L^{2}min). C_i and C_t are concentrations at time t, respectively (mg/L).

The Pseudo-First-Order and Pseudo-Second order models are represented by the equations below:

Pseudo-First-Order, (Darwish, 2015):

$$\ln(q_e - q_t) = \ln(q_e) - tk_1 \quad (2\text{-}16)$$

Where q_e and q_t are the amounts of sulphur adsorbed (mg/g) at equilibrium and at time t (min) respectively. k_1 is the adsorption rate constant (min^{-1}). The values of k_1 can be calculated from the plots of ln $(q_e - q_t)$ versus t for each sorbent material, (Darwish, 2015).

Pseudo-Second-Order, (Darwish, 2015):

$$\frac{t}{q_t} = \frac{1}{{q_e}^2 k_2} + \frac{t}{q_e} \quad (2\text{-}17)$$

Where: k_2 is the equilibrium rate constant in (g/mg.min). The q_e value calculated should match the experimental equilibrium capacity in order for the model process to be pseudo second order. Similarly, values for q_e and k_2 can be determined from the slope and intercept of the plot of t/q_t versus t, (Darwish, 2015).

2.6 Discussion of published adsorption kinetic and isotherm models

2.6.1 Desulphurisation adsorption of diesel fuel onto commercially activated carbon

2.6.1.1 Process Description

Muzic, et al. (2008) studied the desulphurisation of diesel fuel through varies types of commercially available activated carbon. To screen the high performing activated carbon and to carry kinetic characterisation of the adsorption process, experiments were carried out to determine the dependency. Also included in the study was the equilibrium characterisation of the adsorption process. The activated carbons used in this study are listed in Table 1 and they include Chemviron Carbon SOLCARBTM C3, Süd-Chemie G-32H and Norit RGM 3.

Table 1: The activated carbon properties, (Muzic, et al., 2008)

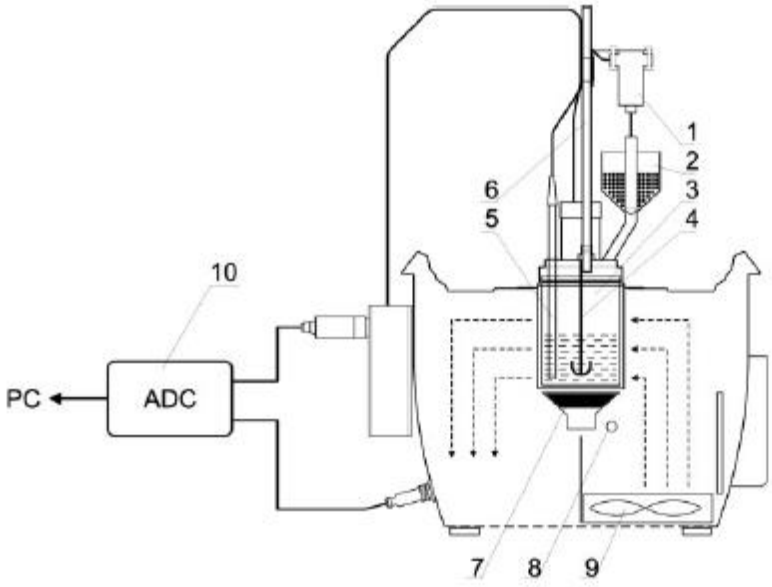
Activated carbon	Units	C3	G-32H	RGM 3
Particle size	mm	1.0-2.0	2.0-5.0	1.0-2.0
Bulk density	$g.cm^{-3}$	0.48	0.5	0.48
Surface area	$m^2.g^{-1}$	936	1100	-
Pore volume	$cm^3.g^{-1}$	0.53	0.75	-

Fuel processed from a conventional hydrodesulphurisation unit with the properties in Table 2 was used in this study.

Table 2: Commercially activated carbon properties, (Muzic, et al., 2008)

Property	Units	Value
Cetane number		51
Cetane index		46
Density at 15°C	kg.m-3	820
Polycyclic aromatic hydrocarbons	wt%	2.1
Total sulphur	mg/kg-1	27
Ignition point	°C	>55
Kinematic viscosity at 40°	mm2.s-1	3.98
Distillation		
distilled up to 250°C	vol. %	<40
distilled up to 300°C	vol. %	75
end of distillation	°C	342

Muzic, et al. (2008) conducted the adsorption process under ambient pressures and at different temperatures ranging from 30–70 °C. The diesel fuel volume used was 50 cm^3 and the absorbers total capacity was 250 cm^3. This experiment was carried in a semiautomatic (which is controlled by a personal computer) laboratory apparatus LAM A1 in Figure 5.



1. Electric valve
2. Adsorbens
3. Adsorber
4. Mixer
5. Temperature sensor
6. Condenser
7. Heater
8. Temperature sensor
9. Ventilator
10. A/D conveter (ADC)

Figure 4: LAM A1 batch adsorption process, (Muzic, et al., 2008).

2.6.1.1.1 Kinetic Study

To enable a better understanding of the adsorption process varies kinetic models were used to test the experimental data. These kinetic model included Pseudo-first order, pseudo-second order and intra-particle diffusion models, it was assumed that the organosulphur concentrations in diesel are very low and thus can be represented as by sulphur concentration as a single component, (Muzic, et al., 2008).

Pseudo-first order, (Muzic, et al., 2008):

$$r_q = k_1(q_e - q) = \frac{dq}{dt} \quad (2\text{-}18)$$

Where: q (mg.g^{-1}) is the amount of sulphur adsorbed at time t (min), k (min^{-1}) is the pseudo-first order adsorption rate constant and q_e is the equilibrium sorption uptake, which is obtained through data extrapolation.

To obtain q_e the experimental data was fitted into equation (2-18) by utilising an Origin software from OriginLab Corp:

$$q = a_o + a_1(1 - (-_{\tau_1}^{t})) + a_2(1 - (-_{\tau_1}^{t})) \quad (2\text{-}19)$$

Where:$a_o, a_1,\ a_2,\ \tau_1, \tau_2$ are mathematically calculated constants. The integrated form of equation (2-19) is:

$$\ln(q_e - q) = \ln(q_e) - k_1 t \quad (2\text{-}20)$$

A linear plot of $\ln(q_e - q)$ versus t is used to determine q_e and k_1.

Pseudo-second order, (Muzic, et al., 2008):

$$r_q = k_2(q_e - q)^2 = \frac{dq}{dt} \quad (2\text{-}21)$$

Where: k_2 (g.mg^{-1}min^{-1}) is the pseudo-second order adsorption rate constant. When integrated equation (2-21) is as follows:

$$\frac{t}{q} = \frac{1}{k_2 q_e^2} + \frac{1}{q_e} t \qquad (2\text{-}22)$$

Where: q_e and k_2 are obtained by plotting t/q versus t.

The intra-particle diffusion model equation is as follows, (Muzic, et al., 2008):

$$q = k_i t^{1/2} + C \qquad (2\text{-}23)$$

Where: k_i is the intra-particle diffusion rate constant (mg.g^{-1}.min$^{-0.5}$) and C (mg.g^{-1}) is the energy of adsorption constant. The intra-particle diffusion model constants can be determined as the slope and intercept of the linear plot of q versus $t^{1/2}$, respectively.

2.6.1.1.2 Adsorption Isotherms

To determine the equilibrium characterisation of the adsorptive desulphurisation process the experimental data was fitted into the Langmuir and Freundlich isotherms. The importance of correlating the experimental data to these isotherms is not only for design and operation purpose but also to reinforce the assumptions that the treatment of adsorptive desulphurization of diesel fuel is a single component adsorption process, (Muzic, et al., 2008).

Langmuir equation, (Muzic, et al., 2008):

$$q = Q_m \frac{K_L}{1 + K_L C_e} \qquad (2\text{-}24)$$

The linear form of equation (2-24) can be expressed as, (Muzic, et al., 2008):

$$\frac{1}{q_e} = \frac{1}{q_{max} K_L} \frac{1}{C_e} + \frac{1}{q_{max}} \qquad (2\text{-}25)$$

Where q is the adsorption capacity of the adsorbent (mg/g), K_L(kg.mg^{-1}) indicates a binding constant which is related to the heat of adsorption and q_{max} is theoretical capacity of the

monolayer. All the constants are specific to experiment conditions and the adsorbent type. The plots of $\frac{1}{q_e}$ versus $\frac{1}{C_e}$ and Log q_e versus Log C_e can be used to test the Langmuir and Freundlich adsorption models, respectively. To determine the adsorption progression, the separation factor R_L was calculated. This factor is expressed as, (Muzic, et al., 2008):

$$R_L = \frac{1}{1+K_L C_0} \quad (2\text{-}26)$$

Where K_L was derived from the Langmuir isotherm and C_0 being the sulphur initial concentration on the diesel fuel. The R_L value indicates the shape of the isotherm to be irreversible *(R_L=0),* favourable *(0< R_L<1),* linear *(R_L=1)* or unfavourable *(R_L>1),* (Muzic, et al., 2008).

Due to the diversity of adsorption sites, the Freundlich isotherm model assumes heterogeneous adsorption, (Muzic, et al., 2008):

$$q = K_F C_e \frac{1}{n} \quad (2\text{-}27)$$

Where: K_F and n are equilibrium adsorption capacity and adsorption intensity constants, respectively. The linear form of equation (2-27) is as follows, (Muzic, et al., 2008):

$$lnq = lnK_F + \frac{1}{n} lnC_e \quad (2\text{-}28)$$

2.6.1.2 Results and discussion

2.6.1.2.1 Kinetic study analysis

SOLCARB C3 was observed to perform better as compared to Sud-Chemie G-32H and Norit RGM 3. The observed adsorbent capacity in Figure 5 is significantly higher for SOLCARB C3 as compared to the other activated carbon.

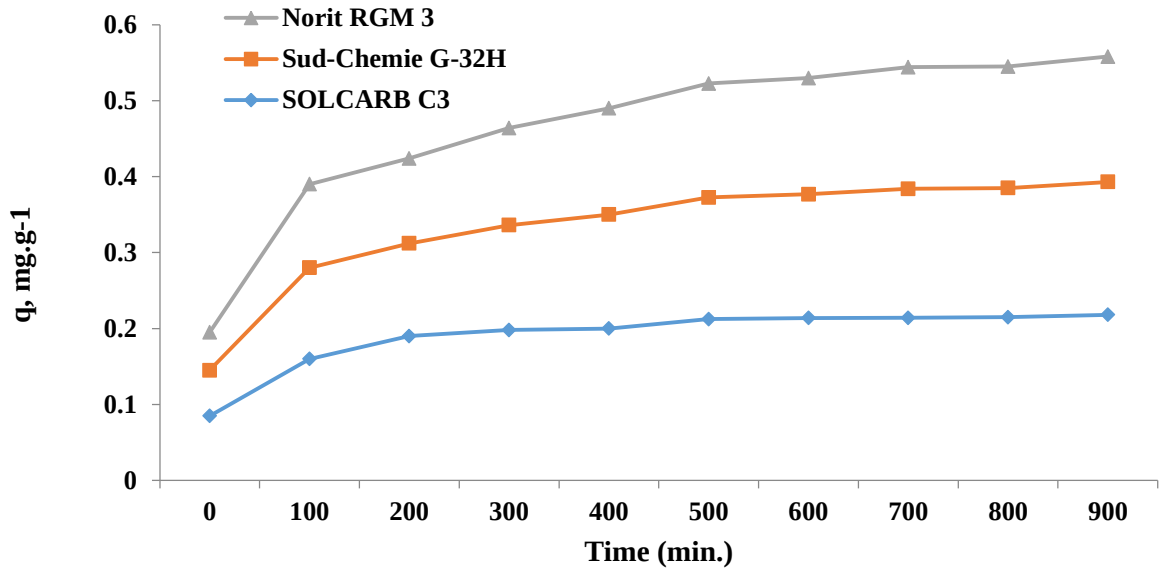


Figure 5: Adsorbent capacity versus time (T=50°C, V_D = 50 cm3, n = 300min^{-1} and $m_{adsobernt}$ = 2g), (Muzic, et al., 2008).

The adsorption kinetics was investigated by applying the pseudo-first order, pseudo-second order and intra-particle diffusion models. The extrapolated results and correlation coefficients are presented in Table 3. For SOLCARB C3 the obtained R squared values were 0.9418 and 0.9994 for pseudo-first order and pseudo-second order, respectively. For Süd-Chemie G-32H the obtained R squared values were 0.9168 and 0.9930 for pseudo-first order and pseudo-second order, respectively. For Norit RGM 3 the obtained R squared values were 0.9288 and 0.9920 for pseudo-first order and pseudo-second order, respectively. These indicate that the diesel fuel adsorptive desulphurisation is best described by the pseudo-second order kinetic model. Furthermore the best pseudo-second order kinetic model was on the SOLCARB C3 activated carbon, which according to Figure 5 performed better as compared to the other adsorbents.

Table 3: Extrapolation results and coefficients of the pseudo-first and pseudo-second order adsorption kinetic models and intra-particle diffusion model., (Muzic, et al., 2008)

Adsorbent	q_e **(mg.g^{-1})**	R^2	
SOLCARB C3	0.2266	0.9965	
Sud-Chemie G-32H	0.2018	0.9765	
Norit RGM 3	0.1874	0.9983	
Pseudo-first order			
Adsorbent	k_1 **(min^{-1})**	q_e **(mg.g^{-1})**	R^2
SOLCARB C3	0.0032	0.0999	0.9418
Sud-Chemie G-32H	0.0014	0.1463	0.9168
Norit RGM 3	0.0013	0.1575	0.9288
Pseudo-second order			
Adsorbent	k_2 **(g.mg^{-1}.min^{-1})**	q_e **(mg.g^{-1})**	R^2
SOLCARB C3	0.1532	0.2261	0.9994
Sud-Chemie G-32H	0.0869	0.1916	0.9930
Norit RGM 3	0.0741	0.1869	0.9920
Intra-particle diffusion model			
Adsorbent	k_i **(mg.g^{-1}.min$^{-0.5}$)**	C_e**(mg.g^{-1})**	R^2
SOLCARB C3	0.0044	0.1012	0.8276
Sud-Chemie G-32H	0.0045	0.0546	0.9259
Norit RGM 3	0.0047	0.0425	0.9314

The adsorption kinetic model is limited by varies mechanism that can include external diffusion, boundary layer diffusion and intra-particle diffusion. Muzic, et al. (2008) included the intra-particle diffusion model to determine the rate limiting mechanism in the carried adsorption experiment. According to Muzic, et al. (2008) if the regression of q versus $t^{1/2}$ is linear and intercepts the origin than intra-particle diffusion is the rate limiting mechanism. In Figure 6 it can be clearly seen that the regression is not linear and did not intercept the origin for any of the investigated activated carbons. Hence the intra-particle diffusion was not the limiting.

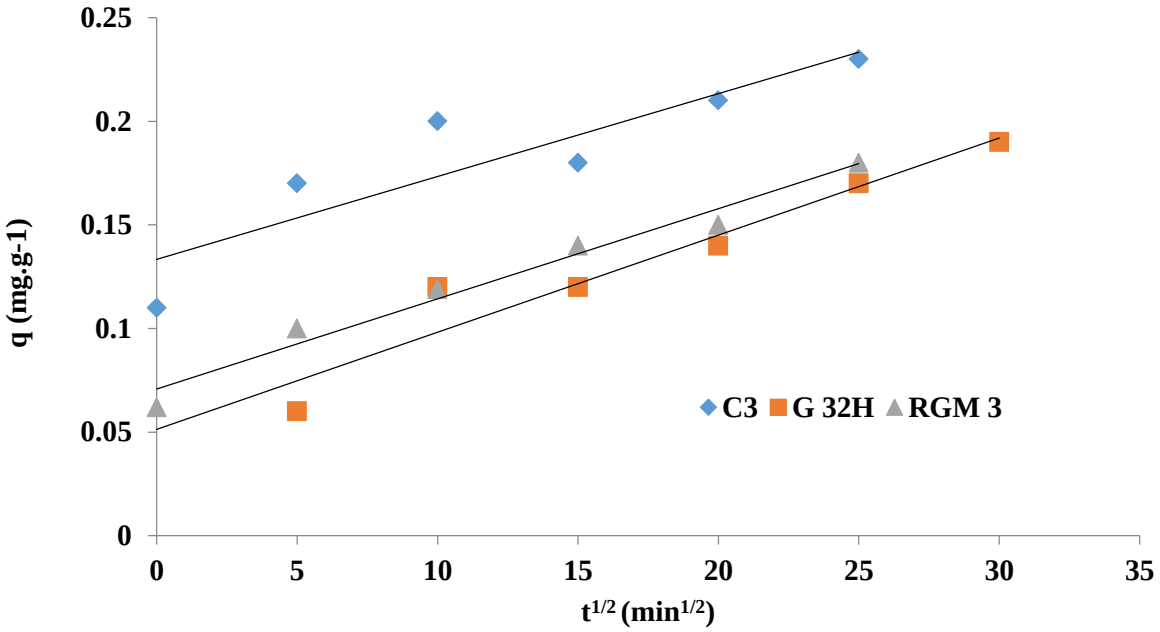


Figure 6: Intra-particle diffusion analysis model, (Muzic, et al., 2008).

2.6.1.2.2 Adsorption equilibrium analysis

It was observed that the SOLCARB C3 equilibrium sorption capacity of > 0.2 $mg.g^{-1}$ was significantly high as compared to that of Sud-Chemie G-32H and Norit RGM 3 at 0.150 $mg.g^{-1}$ and 0.040 $mg.g^{-1}$, respectively. This confirms that the SOLCARB C3 outperformed the other studied activated carbons.

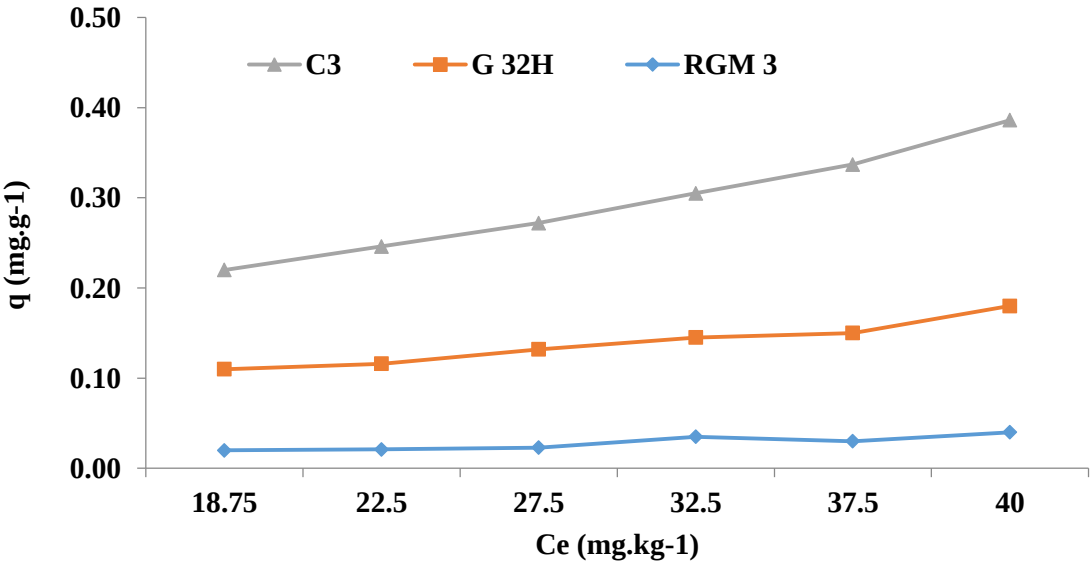


Figure 7: Adsorption isotherms for adsorptive desulfurization of diesel fuel. (Muzic, et al., 2008).

The experiment data fitted the Freundlich model best, the obtained R squared values in Table 4 were 0.9994, 0.9728, 0.9826 for SOLCARB C3, Sud-Chemie G-32H and Norit RGM 3, respectively. The Langmuir R squared values were 0.9500 for Sud-Chemie G-32H & Norit RGM and 0.9734 for SOLCARB C3.

Table 4: Adsorption isotherm constants, correlation coefficients and separation factor, R_L, for the diesel fuel adsorptive desulphurisation, (Muzic, et al., 2008)

Adsorbent	Langmuir isotherm			Freundlich isotherm		
	K_L ($kg.mg^{-1}$)	Q_m ($mg.g^{-1}$)	R^2	K_F	n	R^2
SOLCARB C3	0.0049	1.2640	0.9734	0.0082	1.1362	0.9994
Sud-Chemie G-32H	0.0119	0.4666	0.7500	0.0099	1.3538	0.9728
Norit RGM 3	0.0209	0.0793	0.9462	0.0035	1.5781	0.9826
	C_0 ($mg.kg^{-1}$)					
	18.8	23.2	28.8	34.4	38.4	-
	Seperation Factor, R_L					
SOLCARB C3	0.9143	0.8964	0.8745	0.8536	0.8394	-
Sud-Chemie G-32H	0.8160	0.7823	0.7433	0.7079	0.6847	-
Norit RGM 3	0.7170	0.6725	0.6232	0.5807	0.5537	-

The separation factor, R_L , values in Table 4 were greater than zero but less than one, this is indicative of a favourable adsorption, (Lam and Ridzuan, 2008.). The Freundlich coefficient, *n*, confirmed the favourability with values larger than one, (Okeola and Odebunmi, 2010). Freundlich isotherm best describe physical adsorption, (Castellan, 1983). Muzic, et al. (2008) results confirms that adsorption process on activated carbon are physical in nature (i.e. there is no chemical bond formation).

2.6.2 The desulphurisation adsorption study of thiophene and benzothiophene onto NiCeY zeolites

According to Fei, et al. (2017) simulating the adsorptive removal of sulphur compounds from fuel is the most cost effective approach compared to conducting an experiment. This proactively improves the process efficiency and reduces the experiment cost. Fei, et al. (2017), studied the desulphurisation of thiophene and benzothiophene onto NiCeY zeolites and investigated the isothermal, adsorption kinetics and thermodynamics models on the removal of thiophene and benzothiophene.

NiCeY zeolites were prepared through an ion exchange between NaY with $Ni(NO_3)_2$ and $Ce(NO_3)_3$ solution. Thereafter the adsorption process experiment was conducted from modelled fuels in Table 5 using the NiCeY zeolite. Thiophene, benzothiophene and *n*-octane were used in modelling the diesel fuels with different sulphur concentration and the composition of these fuels is listed in Table 5.

Table 5: The modelled diesel fuel compositions, (Fei, et al., 2017)

Diesel Fuels	Sulphur content (mmol.L-1)	Composition
M1	21.92	Thiophene/n-octane
M2	17.54	Thiophene/n-octane
M3	13.15	Thiophene/n-octane
M4	8.77	Thiophene/n-octane
M5	4.38	Thiophene/n-octane
M6	21.92	Benzothiophene/n-octane
M7	17.54	Benzothiophene/n-octane
M8	13.15	Benzothiophene/n-octane
M9	8.77	Benzothiophene/n-octane
M10	4.38	Benzothiophene/n-octane

Fei, et al. (2017), defines adsorption capacity as follows:

$$q_t = \frac{(C_0 - C_t)V}{m} \qquad (2\text{-}29)$$

Where; V (mL) is the model fuel volume, m (g) is the adsorbent mass, C_0, C_e & C_t (mmol.L^{-1}) is the initial, equilibrium and t (min) sulphur concentration, respectively.

2.6.2.1.1 Kinetic Study

Fei, et al. (2017), studied pseudo-first and pseudo-second order kinetic models.

Pseudo-first order, (Fei, et al., 2017):

$$\frac{dq_t}{dt} = k_1(q_e - q_t) \quad (2\text{-}30)$$

Where: q_t (mmolg^{-1}) is the sulphur adsorption capacity at time t (min), k_1 (min^{-1}) is the rate constant and q_e is the equilibrium capacity. When integrated equation (2-30) deduce to:

$$q_t = q_e(1 - \exp(-k_1 t) \quad (2\text{-}31)$$

Pseudo-second order, (Fei, et al., 2017):

$$\frac{dq_t}{dt} = k_2(q_e - q_t)^2 \quad (2\text{-}32)$$

Where: k_1 (g.mmol^{-1}.min^{-1}) is the rate constant and q_e (mmol.g^{-1}) is the equilibrium capacity. When integrated equation (2-32) deduce to:

$$q_t = \frac{k_2 q_e^2 t}{1 + k_2 q_e} \quad (2\text{-}33)$$

2.6.2.1.2 Adsorption isotherms

In the Langmuir model the interaction between adsorbates and the adsorbent entail two processes, desorption (υ_d) and adsorption (υ_{ads}). The rates can be expressed as:

$$\upsilon_{ads} = k_{ads} c_t (1 - \theta) \quad (2\text{-}34)$$

$$\upsilon_d = k_d \theta \quad (2\text{-}35)$$

Where: k_{ads} and k_d are the desorption and adsorption constants, θ is the adsorbent surface coverage ratio and c_t is the sulphur concentration at time t. θ is represented by q_t/q_m where q_t

is the adsorption capacity at time t and q_m is the equilibrium adsorption capacity. c_e *and* q_e represents the sulphur concentration (c_t) and adsorption capacity (q_t) when the desorption and adsorption rate are equal. Langmuir model is then presented by*:*

$$q_e = \frac{K_L c_e q_m}{1+K_L c_e} \quad (2\text{-}36)$$

Where: K_L represents the Langmuir constant. Both K_L and q_m are calculated from equation (2-35).

The Freundlich isotherm is expressed by:

$$q_e = K_F c_e^{1/n} \quad (2\text{-}37)$$

Where: K_F and n are the Freundlich constant and adsorption intensity, respectively.

2.6.2.2 Results and discussion

2.6.2.2.1 Impact of process parameters

Effect of adsorption temperature: Fei, et al. (2017)**,** observed that the adsorption temperature has two main effects 1. Increasing the temperature resulted in an increase in the diffusion rate of thiophene and benzothiophene in *n*-octane, this is due to the decrease in solution viscosity. 2. If the temperature is too high the adsorption capacity is reduced as this condition enhances the desorption rate.

Effect of resident time (Fei, et al., 2017)**:** To gain an understating of the resident time impact the adsorption experiment was carried at different contact times with the temperature and diesel fuel composition kept the same. It can be seen in Figure 8 that the adsorption capacity increased exponentially in the first 10 min. and thereafter slowed down until equilibrium was reached.

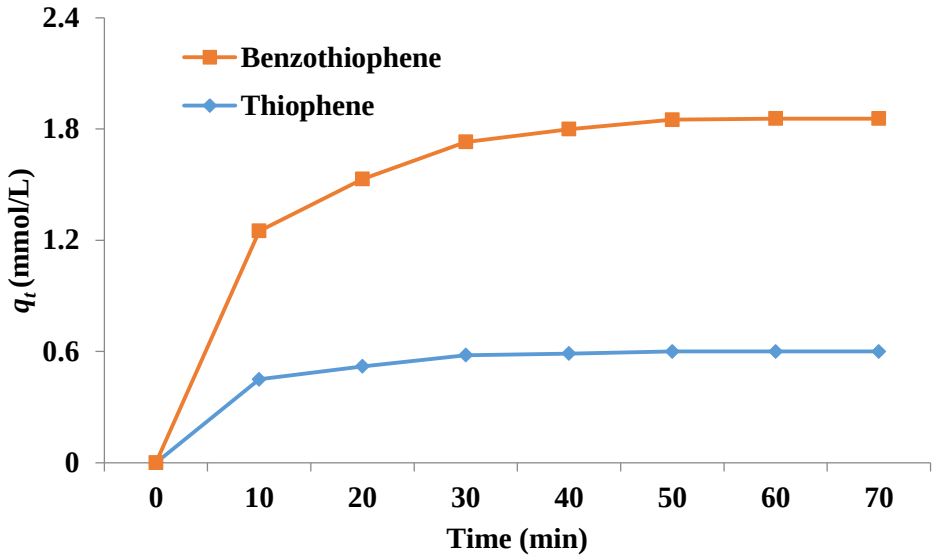


Figure 8: Effect of adsorption time on the removal of thiophene and benzothiophene over NiCeY zeolite, (Fei, et al., 2017).

Effect of initial sulphur concentration: It is shown in Figure 9 that the adsorption capacity was found to vary with initial concentration, an increase in initial sulphur concentration resulted in an increase in adsorption capacity.

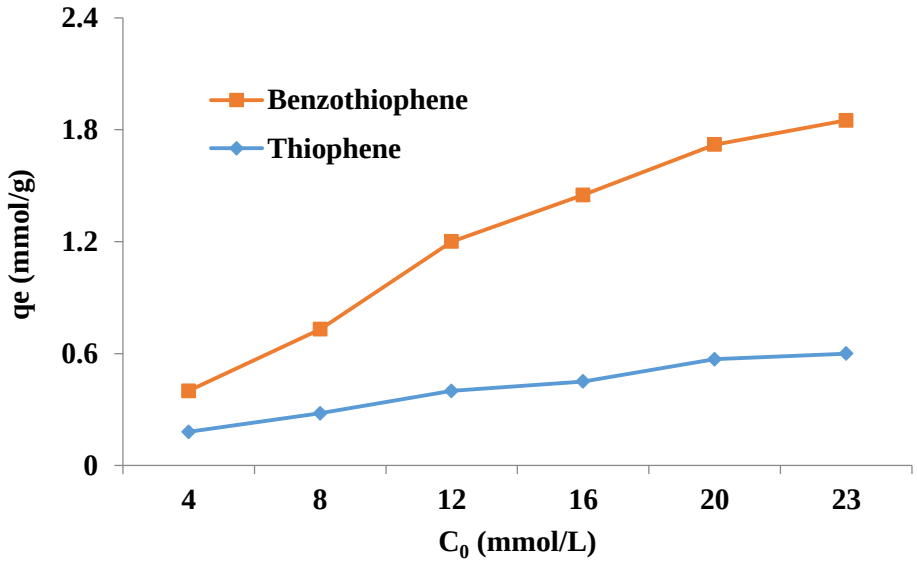


Figure 9: Effect of adsorption time on the removal of thiophene and benzothiophene over NiCeY zeolite, (Fei, et al., 2017).

2.6.2.2.2 Adsorption equilibrium analysis

Fei, et al. (2017) used modelled diesel M1 to M10 with a resident time of 1 hour at temperatures 30, 50 and 70°C in this analysis. The experimental data was fitted into both the Langmuir and Freundlich isotherms. The correlation and calculated parameters at different temperatures are shown in Table 6. The Langmuir constant, $K_{L,}$ was found to increase with an increase in temperature, the thiophene constant increased from 0.085 to 0.128 and the benzothiophene constant increased from 0.175 to 0.330. The maximum adsorption capacities, q_m, also increased with an increase in temperature as seen in Table 6. This confirms that high temperatures are conducive for thiophene and benzothiophene adsorption on NiCeY zeolite. The Langmuir model was found to be the best fit for the thiophene adsorption process, the obtained R squared values at 30, 50 and 70°C were 0.996, 0.995 and 0.994, respectively whereas the obtained R squared values at 30, 50 and 70°C on the Freundlich model (Table 7) were lower at 0.991, 0.991 and 0.988, respectively. This trend was also observed in the adsorption of benzothiophene. Thiophene and benzothiophene are therefore monolayer adsorption on NiCeY zeolites, (Fei, et al., 2017).

Table 6: The Langmuir adsorption isotherm parameters, (Fei, et al., 2017)

	Units	**Parameters**	**30°C**	**50°C**	**70°C**
Thiophene	$mmol.g^{-1}$	q_m	1.030	1.100	1.160
	$L.mmol^{-1}$	K_L	0.085	0.09	0.128
		R^2	0.996	0.995	0.994
Benzothiophene	$mmol.g^{-1}$	q_m	1.820	2.100	2.150
	$L.mmol^{-1}$	K_L	0.175	0.206	0.330
		R^2	0.996	0.997	0.995

Table 7: The Freundlich adsorption isotherm parameters, (Fei, et al., 2017)

	Units	**Parameters**	**30°C**	**50°C**	**70°C**
Thiophene		n	1.570	1.590	1.780
	L mmol-1	K_L	0.116	0.128	0.158
		R^2	0.991	0.991	0.988
Benzothiophene		n	1.600	1.660	1.860
	L mmol-1	K_L	0.358	0.398	0.473
		R^2	0.957	0.958	0.965

2.6.2.2.3 Kinetic study analysis

Fei, et al. (2017) studied the pseudo-first order and pseudo-second order kinetic models. As seen in Table 8 & Table 9 both kinetic models fitted the experimental data well however the pseudo-first order model's R squared value was found to be less as compared to that of the pseudo-second order which was > 0.990. Thus pseudo-second was the best fit for the adsorption of thiophene and benzothiophene over NiCeY zeolite.

Table 8: The pseudo-first order experimental data fitting at 30, 50 & 70°C, (Fei, et al., 2017)

	Units	**Parameters**	**30**°C	**50°C**	**70°C**
Thiophene	min^{-1}	K_1	0.225	0.235	0.247
	$mmol.g^{-1}$	q_e	0.620	0.650	0.680
		R^2	0.972	0.969	0.982
Benzothiophene	min-1	K_1	0.127	0.165	0.243
	$mmol.g^{-1}$	q_e	1.230	1.250	1.280
		R^2	0.975	0.987	0.982

Table 9: The pseudo-second order experimental data fitting at 30, 50 &70°C, (Fei, et al., 2017)

	Units	**Parameters**	**30**°C	**50°C**	**70°C**
Thiophene	$g.mmol^{-1}.min^{-1}$	K_1	0.519	0.493	0.553
	$mmol.g^{-1}$	q_e	0.670	0.720	0.730
		R^2	0.993	0.992	0.997
Benzothiophene	$g.mmol^{-1}.min^{-1}$	K_1	0.140	0.158	0.282
	$mmol.g^{-1}$	q_e	1.370	1.390	1.400
		R^2	0.996	0.999	0.997

Fei, et al. (2017) also investigated the effect that temperature has on the adsorption kinetics. As discussed in section 2.6.2.1.1 the effect of temperature on the adsorption process is mainly 1. There is a direct correlation between adsorption temperature and rate of diffusion, an increase in temperature will result in an increase in diffusion rate of the adsorbate in the solution. This is due to the decreased solution velocity. 2. A temperature change will shift the equilibrium adsorption capacity of the zeolites. The effect of temperature on the adsorption capability is shown in Figure 10.

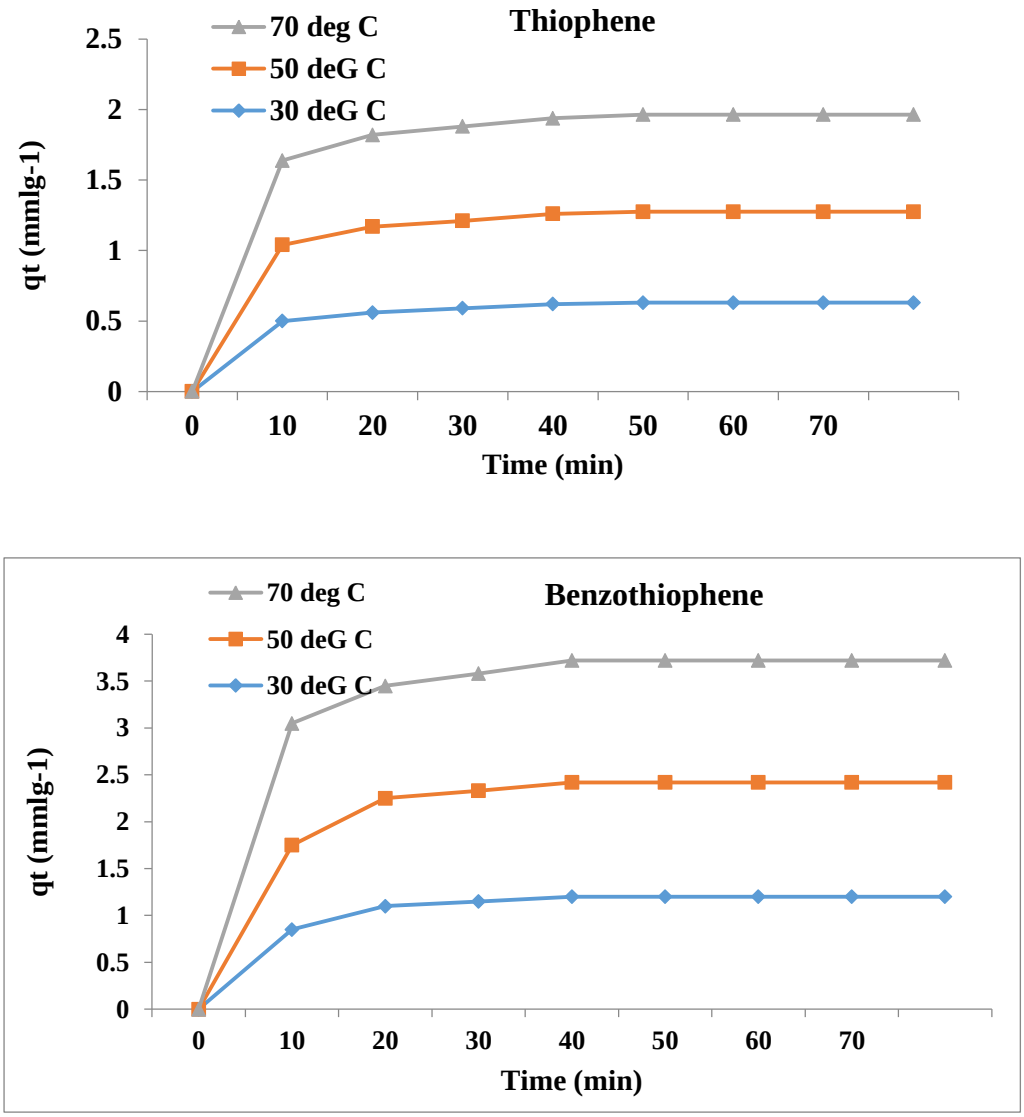


Figure 10: The effect of temperature on the adsorption of thiophene and benzothiophene over NiCeY zeolite, (Fei, et al., 2017).

2.6.3 The desulphurisation adsorption of dibenzothiophene in model diesel fuel on carbonaceous materials loaded with aluminium oxide particles

Nazal, et al. (2015) studied the nature and kinetics of adsorption of dibenzothiophene in model diesel fuel on carbonaceous materials loaded with aluminium oxide particles. The carbonaceous materials used as adsorbents were commercial activated carbon (AC), multiwall carbon nanotubes (CNT) and synthesized graphene oxide (GO). To improve the chemical properties of the adsorbent surface these material were loaded with 5% and 10.9 % of aluminium (AL) in the form of aluminium oxide (Al_2O_3). The resulting adsorbents are

represented by ACAL5 (activated carbon loaded with 5% Al_2O_3), ACAL10 (activated carbon loaded with 10% Al_2O_3), CNTAL5 (activated carbon loaded with 5% Al_2O_3), CNTAL10 (activated carbon loaded with 5% Al_2O_3), GOAL5 (activated carbon loaded with 5 % Al_2O_3) and GOAL10 (activated carbon loaded with 10% Al_2O_3.

The adsorption process of dibenzothiophene on impregnated AC, CNT and GO was performed in a batch mode experiment at 25°C and a speed of 200 rpm. To enable studying the adsorption kinetics a solution of dibenzothiophene at different concentrations of n-hexane was used a model fuel.

2.6.3.1.1 Adsorption isotherms

Nazal, et al. (2015) also states that the Langmuir model assume identical adsorption sites with no interaction amongst molecules on neighbouring sites, hence homogenous adsorption.

Langmuir model, (Nazal, et al., 2015):

$$q_e = \frac{Q_{max} b C_e}{1 + b C_e} \quad (2\text{-}38)$$

Where: Q_{max} (mg.g^{-1}) is the maximum capacity, b is the Langmuir constant and C_e (mg.L^{-1}) is the equilibrium sulphur concentration. Equation (2-38) can be linearized to:

$$\frac{C_e}{q_e} = \frac{1}{b Q_{max}} + \frac{C_e}{Q_{max}} \quad (2\text{-}39)$$

The Freundlich model assumes a heterogeneous multi-layer adsorption capacity, (Castellan, 1983).

Freundlich model, (Nazal, et al., 2015):

$$q_e = K_F C_e^{1/n} \quad (2\text{-}40)$$

Where: K_F and n are Freundlich constant and measure of heterogeneity of the adsorbent surface, respectively. When linearized equation (2-40) become:

$$ln q_e = ln K_F + \frac{1}{n} ln C_e \quad (2\text{-}41)$$

Q_{max} was obtained from the linear plot of C_e/q_e versus lnC_e (equation (2-38)). The heterogeneity measure n was obtained from the slope of the linear least fit of lnq_e versus lnC_e (equation (2-40)) whilst the K_F value was obtained from this plot's intercept.

2.6.3.1.2 Kinetic Study

The adsorption results were fitted into pseudo-first order, pseudo-second order and intra-particle diffusion models.

Pseudo-first order model, (Nazal, et al., 2015):

$$\ln(q_e - q_t) = lnq_e - k_1 t \quad (2\text{-}42)$$

Pseudo-second order model, (Nazal, et al., 2015):

$$\frac{t}{q_t} = \frac{1}{q_e^2 k_2} + \frac{t}{q_e} \quad (2\text{-}43)$$

Where: q_e ($mg.g^{-1}$) is the equilibrium adsorption capacity, q_t ($mg.g^{-1}$) is the adsorption capacity at time t (min), k_1 (min^{-1})) is the pseudo-first order rate constant and k_2 ($g.mg^{-1}.min^{-1}$) is the is the pseudo-second order rate constant.

2.6.3.2 Results and discussion

2.6.3.2.1 Adsorption equilibrium analysis

According to Nazal, et al. (2015) larger n and K_F values are an indication of a greater heterogeneity and adsorption capacity, respectively. As shown in Table 10, the adsorbent n values did not change significant with a change in adsorbent. These values ranged between 1.2 and 1.9, this is an indication of dibenzothiophene adsorption tendencies. The K_F value was found to increase with modified adsorbents, which is indicative of higher adsorption capacity for dibenzothiophene molecules compared to the unmodified adsorbents. The R squared values for the Freundlich model were found to be slightly greater than those of the Langmuir in all the studied adsorbents, thus the experiment data bet fitted the Freundlich model and adsorbent surface is heterogeneous with a multi-layer adsorption capacity, (Nazal, et al., 2015).

Table 10: Langmuir and Freundlich parameters and correlation coefficient for dibenzothiophene on carbonaceous materials, (Nazal, et al., 2015)

Adsorbent	Freundlich			Langmuir		
	n	K_F $(mg^{(1-1/n)}mg^{-1}L^{1/n})$	R^2	Q_{max} $(mg.g^{-1})$	***b*** $(dm^3.mg^{-1})$	R^2
AC	1.7 ± 0.1	4.9±0.5	0.9747	42 ±3	$(1.1±0.1)x10^{-1}$	0.9795
CNT	1.69 ±0.04	$(8.9±0.5)x10^{-1}$	0.9968	24 ±2	$(1.5±0.1)x10^{-2}$	0.9702
GO	1.22 ±0.05	$(1.2±0.2)x10^{-1}$	0.9912	23±3	$(3.0±1.0)x10^{-3}$	0.9201
ACAL5	1.29 ±0.08	4.94±0.04	0.9821	70±3	$(4.7±0.2)x10^{-2}$	0.8503
CNTAL5	1.26 ±0.04	6.3±0.2	0.9953	85±1	$(7.8±0.3)x10^{-2}$	0.9603
GOAL5	1.93 ±0.04	2.5±0.1	0.9982	33±4	$(3.4±0.2)x10^{-2}$	0.9395
ACAL10	1.55 ±0.05	1.6±.01	0.9973	41±4	$(2.1±0.01)x10^{-2}$	0.9450
CNTAL10	1.49 ±0.05	$(3.0±0.3)x10^{-1}$	0.9935	16±2	$(7.3±0.1)x10^{-3}$	0.9571
GOAL10	1.4 ±0.01	$(4±1)x10^{-1}$	0.9562	29±9	$(6.1±0.9)x10^{-3}$	0.5310

The Q_{max} trend (Table 10) in the dibenzothiophene adsorption on AC, ACAL5 and ACAL10 was ACAL5 > ACAL10 > AC and Q_{max} for CNT, CNTAL5 and CNTAL10 followed the same trend as it was observed that CNT5 > CNTAL10 > CNTAL10. The adsorption on GO Q_{max} findings were different, GOAL5 > GO > GOAL10. The Q_{max} values for the Ac adsorbents were found to be higher than the CNT and GO. It was also found that there was no significant different in the Q_{max} of the different GO adsorbents and Nazal, et al. (2015) contributes this to the possibility of agglomeration of the graphene oxide layers after there were impregnated with the aluminum.

The increase in Q_{max} with an increase in loaded Aluminum is as a result of an introduction of an additional acidic adsorption site on the carbon surface rather than increase in surface area and pore volume, (Nazal, et al., 2015). Nazal, et al. (2015) further concludes that the unsaturated surface of Al_2O_3 acts as a Bronsted acid and Lewis acid.

2.6.3.2.2 Kinetic study analysis

The initially fast adsorption shown in Table 11 is credited to the large number of active site at the beginning of the experiment. As more sites are used the absorption capacity slows down and equilibrium is reached. The linear square fit (R squared value) of $\ln(q_e-q_t)$ versus t yielded low correlation coefficients which were not reported in Nazal, et al. (2015)'s study, however the linear square fit of $1/q_t$ versus t yielded correlation efficiencies were close to 1. There was also marginal difference observed in the experimental adsorption capacity and the predicted capacity shown in Table 5. Thus the best fit was the pseudo-second order model.

Table 11: Pseudo-second order kinetic parameters for dibenzothiophene adsorption of the carbonaceous materials impregnated with Al_2O_3, (Nazal, et al., 2015)

Adsorbent	Pseudo-second order parameters			
	$q_{e,\ experiment}$ (mg.g^{-1})	$q_{e,\ predicted}$ (mg.g^{-1})	k_2 (g.mg^{-1}.min^{-1})	R^2
ACAL10	39.3	38.7±0.2	0.015±0.002	0.9999
CNTAL10	23.4	23.4±0.1	0.09±0.02	1.0000
GOAL10	9.4	9.5±0.2	0.035±0.02	0.9981
ACAL5	39.2	39.1±0.1	0.033±0.004	1.0000
CNTAL5	25.4	25.7±0.3	0.02±0.01	0.9993
GOAL5	16.8	16.8±0.1	0.15±0.07	0.9999

2.7 Mass transfer in adsorption packed bed

The concept of a breakthrough curve describes the performance of a packed bed, Shaverdi, 2012. This concept is defined as the point at which a desired effluent concentration is reached, it is also a good indication that the adsorbent has been exhausted and requires replacement, Shaverdi, 2012. In this curve the concentration at a fixed point in the bed is plotted against time. Alternatively a dimensionless plot of effluent concentration (C_e) divided by the inlet concentration (C_{in}) can be plotted against time (i.e. C_e/C_{in} versus time) such that the vertical axis range between zero and one. With one being reached when the bed is exhausted, (Shaverdi, 2012).

The shape and appearance of the breakthrough curve is critical in predicting the operation and dynamic response of an adsorption process, (Goud, et al., 2005).

2.7.1 Mass transfer Zone

The bed length at which the adsorption process takes place is referred to as a mass transfer zone (MTZ), it moves along the bed as the adsorption process progresses. As the adsorbent in the MTZ reaches equilibrium capacity (i.e. becomes exhausted), the MTZ travels further through the bed leaving a section of exhausted adsorbent behind and fresh adsorbent particle leading in front. The breakthrough curve is reached when the front edge of the MTZ reaches the end point of the bed, refer to Figure 11 for a demonstration.

The MTZ length is a function of inlet flow rate and adsorption rate. The effluent concentration will not be zero if the MTZ length is longer than that of the adsorbent bed. According to (Shaverdi, 2012) the MTZ is not instantaneous it is formed over time. The time required to form MTZ is referred to as formation time. If the residence time through the bed is longer than the MTZ formation time, the effluent concentration will also not start at zero. The MTZ length and velocity are therefore two critical parameters during the design of adsorption bed. There is a trade-off between MTZ length and adsorption capacity, minimizing the MTZ length increases the bed capacity.

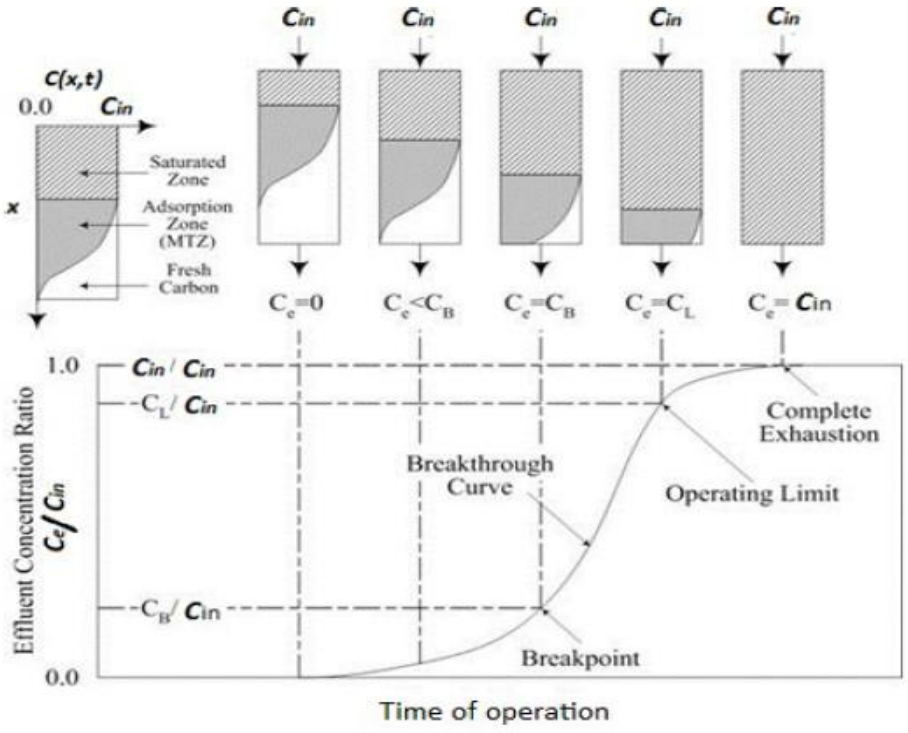


Figure 11: Mass transfer zone movement demonstration through an activated carbon bed and the resulting breakthrough curve, (Shaverdi, 2012).

2.7.2 Stages of Mass transfer

According to Shaverdi (2012) there are three stages taking place during the transfer of adsorbate molecules in the fluid onto the adsorbent and these stages occur in series. These stages are discussed in detail below.

2.7.3 External transport

This stage entails the transfer of molecules from the bed bulk flow to the particle surface via convection. According to the linear Fick's law this stage is represented by the film coefficient h_m.

$N_a = h_m(C - C^*)$

Where:

N_a in the mass flux

h_m is the convective mass transfer

C is the bulk concentration

C^* is the concentration at the particle surface

Wakao *et al*, 1978 proposes that h_m can be obtained from the correlation between Re and Sc numbers using eqn x:

$$Sh = 1.1\ Re^{0.6}\ Sc^{1/3} + 2 \tag{2-44}$$

Where *Sh*, *Re* and *Sc* are defined as:

$$Re = \frac{u_s.d_p}{v} \tag{2-45}$$

$$Sh = \frac{h_m.d_p}{D_m} \tag{2-46}$$

$$Sc = \frac{v}{D_m} \tag{2-47}$$

Where:

u_s is superficial velocity

dp is the pellet diameter

Dm is the molecular diffusivity

v kinematic viscosity

2.7.4 Internal transport

In this step the molecules are adsorbed onto the internal adsorbent structure as they penetrate into the porous adsorbent structure. It is through pore and surface diffusion that this step occurs. In mathematical modelling understanding the process and physical properties can assist in simplifying the proposed model, (Shaverdi, 2012). Model development is differentiated by the different transfer condition assumptions through which mass transfer occurs such as homogenous surface diffusion model, pore diffusion, pore surface diffusion etc.

Pore Diffusion: In this process particles diffuse through the particle pores and the rate is dependent of pore size. There is molecular diffusion which is as a result of molecule collision against each other and Knudsen diffusion which occur due to molecule collision with the pore walls.

***Surface Diffusion*:** In this mechanism molecules jump from site to site. Consequently the type of diffusivity is strongly dependent on the surface concentration and the fractional surface coverage. If the surface area and concentration are high this mechanism will be dominant. This mechanism has proved to be high in adsorptive gas separation processes.

3 MODELLED EXPERIMENT DATA

The data used was obtained from a study performed by Fadhel (2010). The objective of Fadhel (2010)'s study was to investigate the feasibility of deep desulphurisation of light oil and diesel fuel using a polymer supported imidation agent as an adsorbent. Two adsorbents were investigated, Synthesised PI and Chloramine T. The effect of initial sulphur concentration on the desulphurisation efficiency was also investigated.

3.1 Chloramine T and Synthesised PI as adsorbents in model light oil desulphurisation

Light oil was modelled by using an N-tetradecane solution containing 11 mmol/l of DBT. This corresponds to an initial sulphur content of 0.05 wt% (500ppm). The model light oil was reacted with reaction chloramine T (used as an adsorbent) in the presence of MeOH and AcOH at constant temperature of 323 K.

It was found that the sulphur concentration in model light oil (DBT in n-tetradecane) decreased with time, Figure 12. The analysis showed that complete sulphur removal efficiency is achievable after 6hrs of reaction, the sulphur concentration in model light oil was found to be 0 ppm. Fadhel (2010)'s findings agrees with Yasuhiro, et al. (2002) findings. Yasuhiro Shiraishi (2002) obtained a complete sulphur compounds removal after 4 hours of reaction.

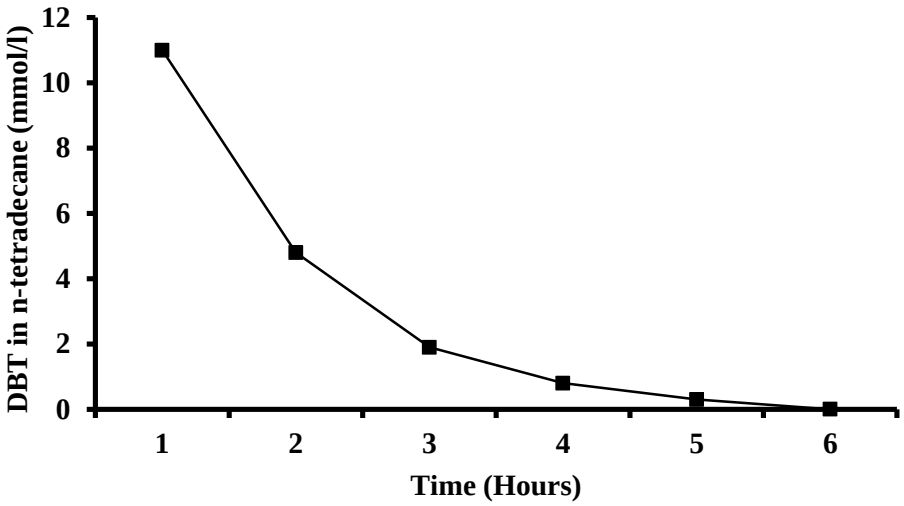


Figure 12: Model light oil sulphur concentration as function of time, using Chloramine T as an adsorbent, Fadhel, 2010

A complete removal was also achieved with Synthesised PI as an adsorbent. However the complete removal was achieved after 8hrs of residence time instead of the 6hrs achieved when Chloramine T was used, Figure 13, (Fadhel, 2010). This implies that the rate of removal with Synthesis PI is slow as compared to that of Chloramine T.

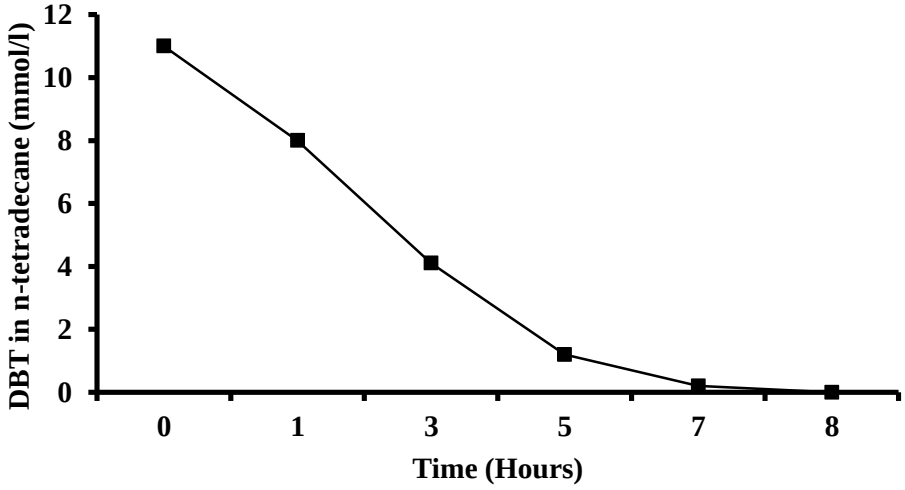


Figure 13: Model light oil sulphur concentration as function of time, using Synthesis PI as an adsorbent, (Fadhel, 2010)

3.2 Chloramine T and Synthesised PI as adsorbents in diesel oil desulphurisation

To study the feasibility of deep desulphurisation in diesel, Fadhel, 2010 utilised two commercial diesel oils from Al-Dura and Beji Refinery with the following properties:

Table 12: Properties of the diesel fuel, (Fadhel, 2010)

Property	Units	Al-Dura Refinery (Diesel fuel 1)	Beji Refinery (Diesel fuel 2)
Specific gravity @15.6 °C	g/cm^3	0.865	0.834
Flash Point	°C	108	105
API		31.9	37.4
Sulphur Content	wt%, ppm	1.23, 12354	0.19, 1900

The findings showed that deep desulphurisation cannot be achieved with using both Chloramine and Synthesised PI. Deep desulphurisation is defined as diesel with a sulphur content of less 500 ppm.

3.2.1 Chloramine T as an adsorbent in diesel oil desulphurisation

Desulphurisation was achieved in both diesel oils however the rate of desulphurisation proved to be faster with Diesel fuel 1 which has a higher initial concentration of 12354ppm as compared to that of diesel fuel 2 with an initial sulphur content of 1900ppm, Figures 14 and 15. Equilibrium was reached after 12 and 20 hours in Diesel fuel 1 and 2 respectively. According to Fadhel (2010), the low desulphurisation efficiency in diesel fuel 2 may be due to the DBT's low polarity sulfimides, which have large carbon number of substituents that are formed by the reacting with chloramine T.

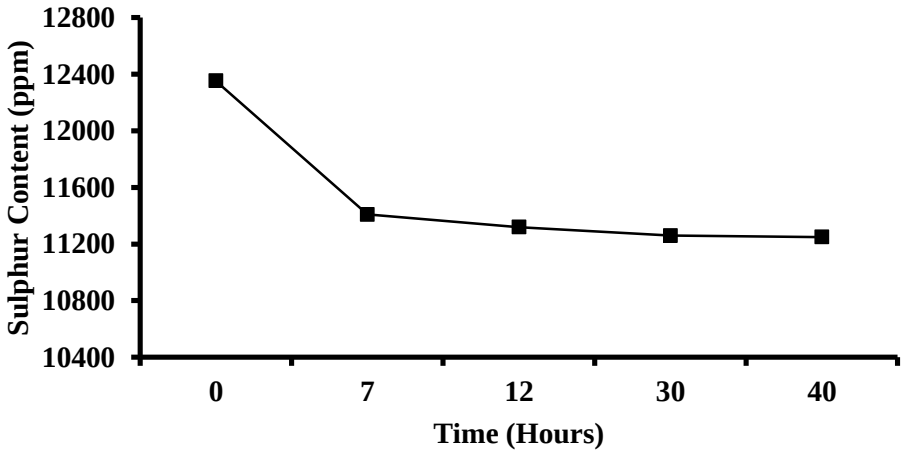


Figure 14: Diesel fuel 1 sulphur content as function of time, using Chloramine T as an adsorbent, (Fadhel, 2010)

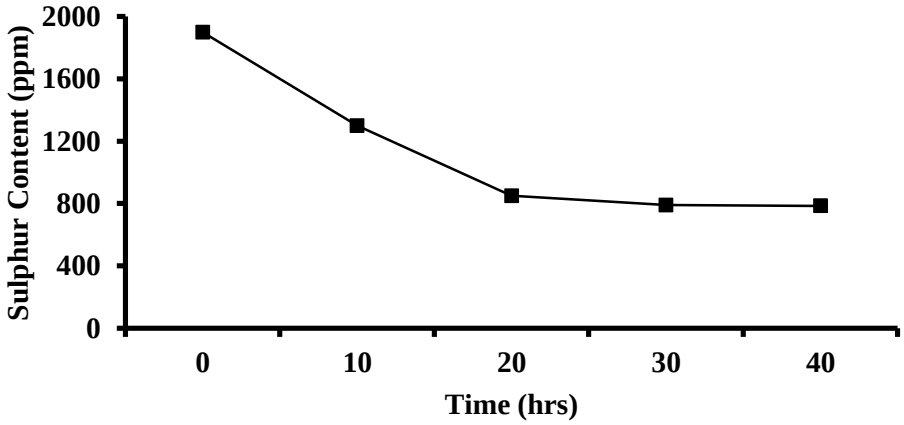


Figure 15: Diesel fuel 2 sulphur content as function of time, using Chloramine T as an adsorbent, (Fadhel, 2010)

3.2.2 Synthesised PI as an adsorbent in diesel oil desulphurisation

Figures 16 and 17 show the correlation between Sulphur content in the diesel oils and reaction time. Desulphurisation was achieved but removal did not reach deep desulphurisation level.

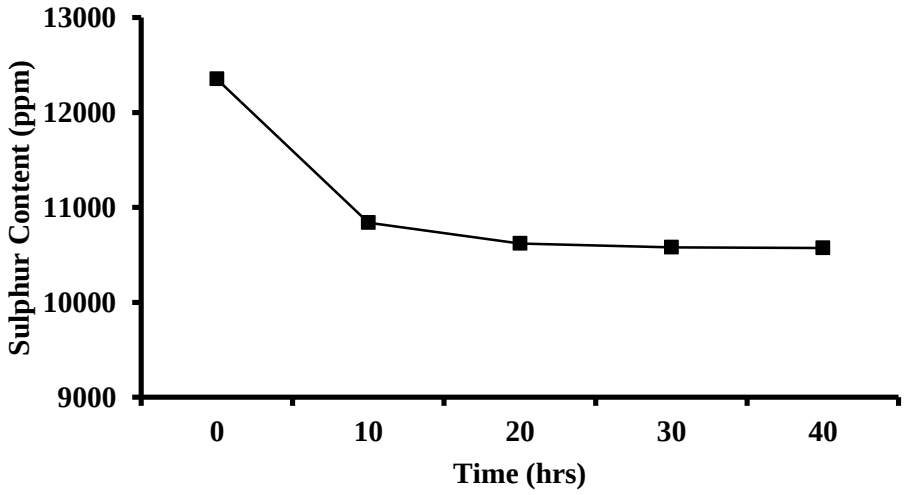


Figure 16: Diesel fuel 1 sulphur content as function of time, using Synthesis PI as an adsorbent, Fadhel, 2010

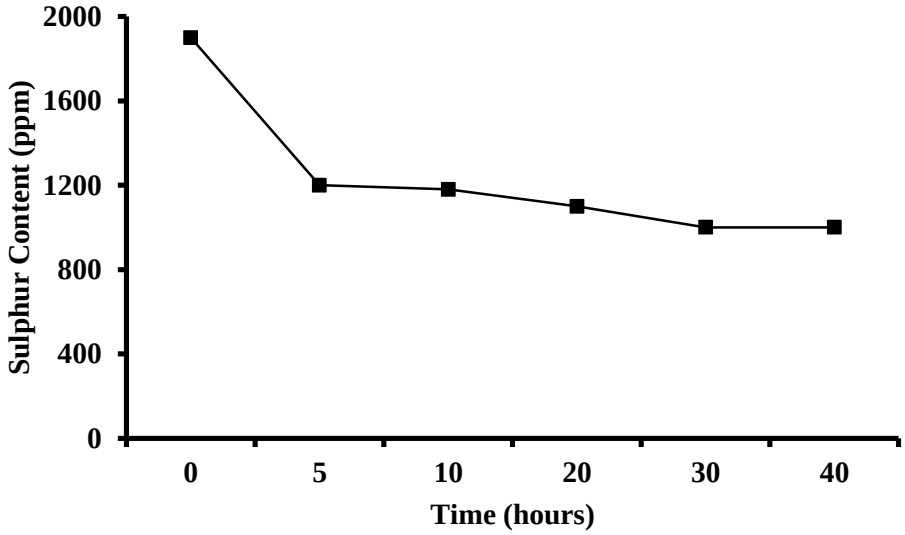


Figure 17: Diesel fuel 2 sulphur content as function of time, using Synthesised PI as an adsorbent, (Fadhel, 2010)

3.3 Investigated optimal operating conditions

Fadhel (2010) further investigated the impact of the residence time, initial sulphur concentration in adsorbate and adsorbent dose has on the desulphurisation efficiency and rate. The objective of this was to determine the process' optimal operation conditions.

Figure 18 show that there is a linear correlation between the desulphurisation efficiency and adsorbent dose (i.e. the high the dose the more sulphur is removed from the diesel oil and vice versa). The increase in desulphurisation efficiency is due to the increase in adsorbent surface area (i.e. more active site availability for adsorption).

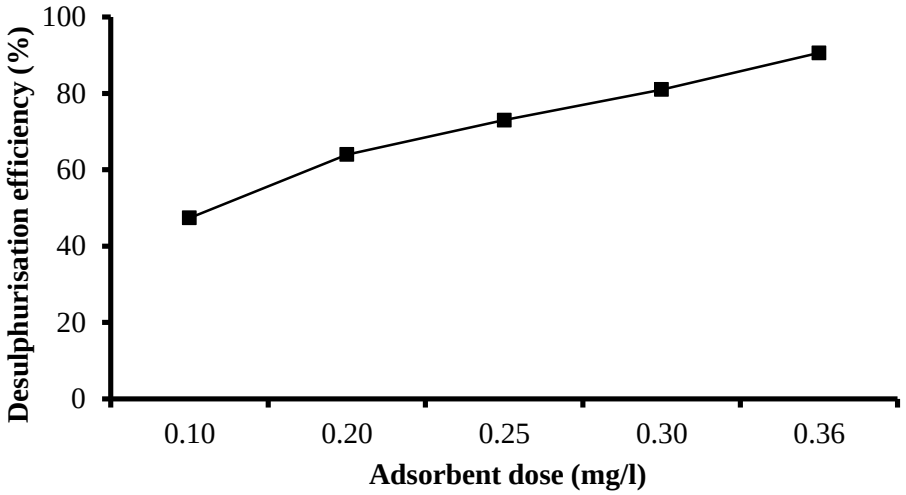


Figure 18: Desulphurisation efficiency as function of adsorbent dose at t = 40 hrs and C_0 = 1900ppm in Diesel fuel 2, (Fadhel, 2010)

Fadhel (2010) also found that at adsorbent doses beyond 0.25 mg/l, deep desulphurisation (Sulphur content <500ppm) is feasible, Figure 19.

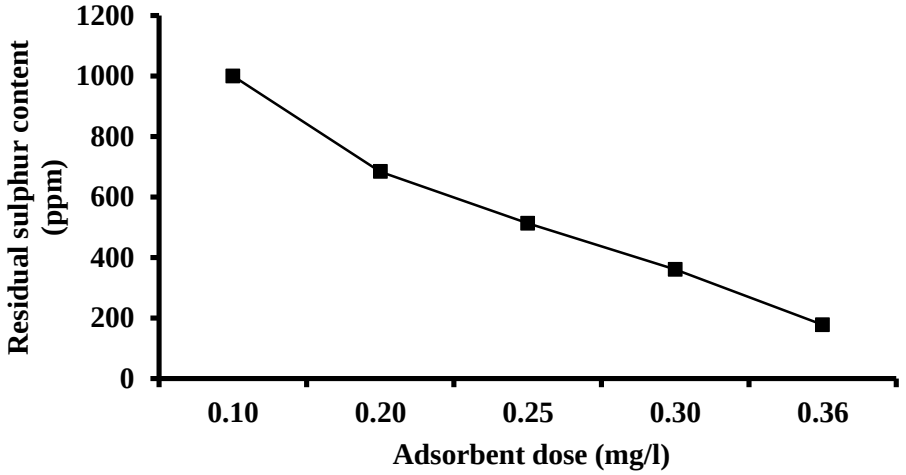


Figure 19: Residual sulphur content as function of adsorbent dose at t = 40 hrs and C_0 = 1900ppm in Diesel fuel 2, (Fadhel, 2010)

The desulphurisation efficiency as shown in Table 13 was found to be high with low initial sulphur content hence the efficiency was higher in Diesel fuel 2 which had an initial sulphur content of 1900ppm as compared to that of Diesel fuel 1 with an initial concentration of 12354ppm, (Fadhel, 2010). Nazal, et al. (2015) attribute this to the large number of active site at the beginning of the experiment or ate low concentrations and as more sites are used up the absorption capacity slows down and equilibrium is reached.

Table 13: Desulphurisation efficiency as function of initial sulphur concentration

C_0 (ppm)	Ƞ (%)
1900	90.63
12354	14.35

4 ADSORPTION ISOTHERM AND KINETICS ANALYSIS

4.1.1 Analysis Technique

Fadhel (2010)'s experimental data was fitted into the studied adsorption isotherms and kinetics models. Regression analysis was thereafter used to examine how well the data fitted the models. Regression analysis is a statistical tool used to validate correlations between variables by generating an equation that describe a statistical relationship between the dependent and independent variable (i.e. assist in understanding how the dependent variable changes with a change in the independent variable). The following statistical variables were used to evaluate the relationship, Minitab, n.d.

- **R Square -** This variable always range between 0 and 100% (i.e. 0 to 1), it indicate how accurate the regression estimates the actual data. A higher value indicates a better model fit, the higher the R square value the better the model will fit the data.
- **Standard Error** – Measures the average distance between the observed values and the regression line this indicates the accuracy of the regression model. A smaller error indicates that the observations are closer to the fitted line.
- **Residual Output –** Measures the difference between the observed value of the dependent variable (y) and the predicted value ($\hat{y}$)

  $$\text{Residual} = \text{Observed value} - \text{Predicted value}$$

  In a residual plot the residuals were plotted on the vertical axis and the independent variable on the horizontal axis. If the points in a residual plot are randomly dispersed around the horizontal axis, it is an indication of a good fit for linear regression model otherwise a non-linear model is more appropriate.

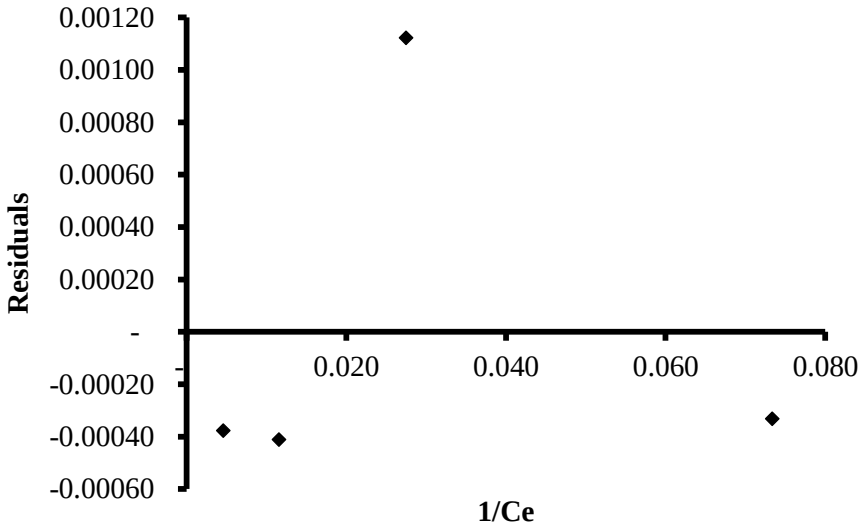
4.1.2 Analysis Results

4.1.2.1 Adsorption Isotherms

4.1.2.1.1 Chloramine T as an adsorbent in model light oil desulphurisation

The obtained R squared values were 0.993 and 0.995 for Langmuir and Freundlich respectively. This indicated that both the Langmuir and Freundlich isotherm models were best describing the removal process. However the standard error was slightly higher for the Freundlich isotherm, 0.038 as compared to 0 in the Langmuir model.

The residual and line plot confirmed the observed best fits, the values of $1/q_e$ & log q_e predicted through linear regression were in-line with the experimental data values, refer to Figure 20 and 21.



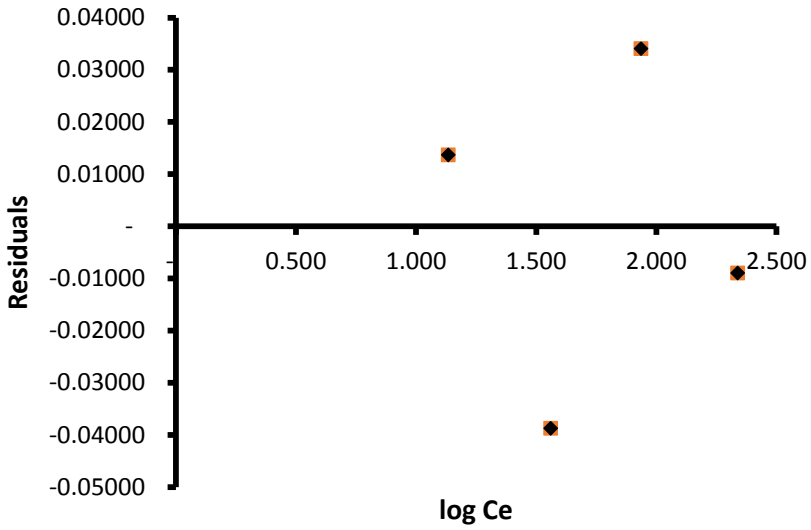
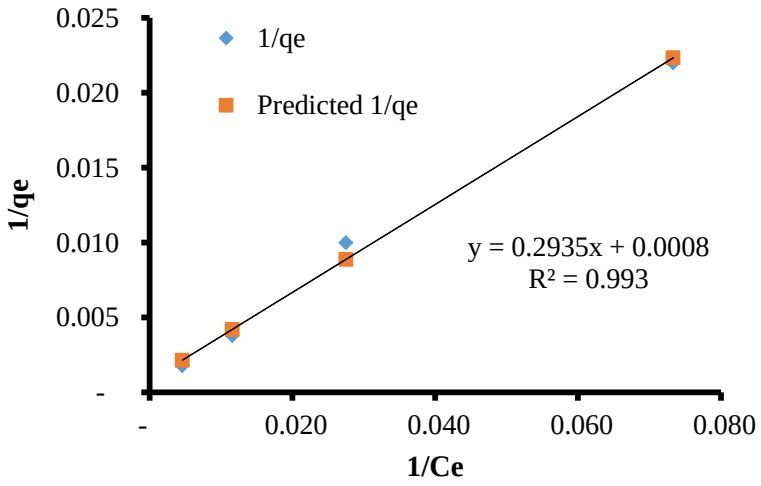


Figure 20: 1/qe and log qe residual plots respectively



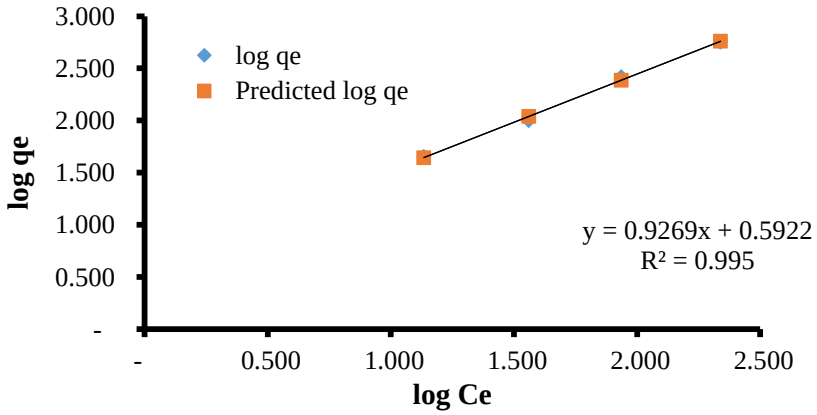


Figure 21: 1/qe and log qe line fit plots respectively

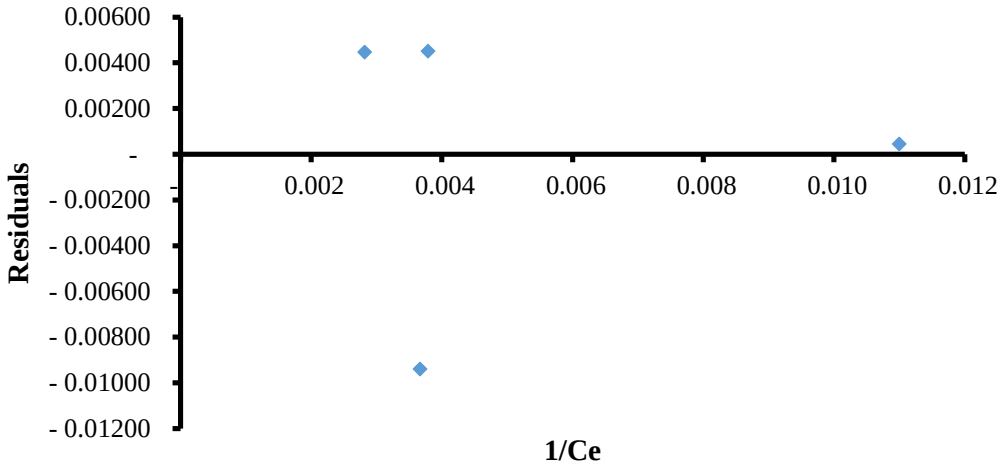
The calculated Langmuir separation factor R_L was 0.25 which according to, Lam and Ridzuan (2008)'s defination if $0<R_L<1$ the Langmuir isotherm is favourable. In the Freundlich isotherm the obtained adsorption strength constants (1/n) was 0.936. According to Okeola (2010) a high 1/n value is an indication of a strong adsorption bond, at <1 this Isotherm also confirmed that the adsorption was slightly favourable.

The model findings confirmed the favourability of the adsorption process as complete desulphurisation was achieved in the conducted experiment.

4.1.2.1.2 Synthesised PI as an adsorbent in model light oil desulphurisation

The experiment data fitted the Langmuir model the best, the obtained R squared values were 0.983 and 0.778 for Langmuir and Freundlich models respectively. The standard error in the Freundlich model was higher at 0.151 as compared to that of 0.0006 in the Langmuir.

The residual and line fit plot also confirmed the best fit to be the Langmuir model, the deviation between the predicted and observed dependent variable was negligible in the Langmuir as compared to the Freundlich, refer to Figures 22 and 23.



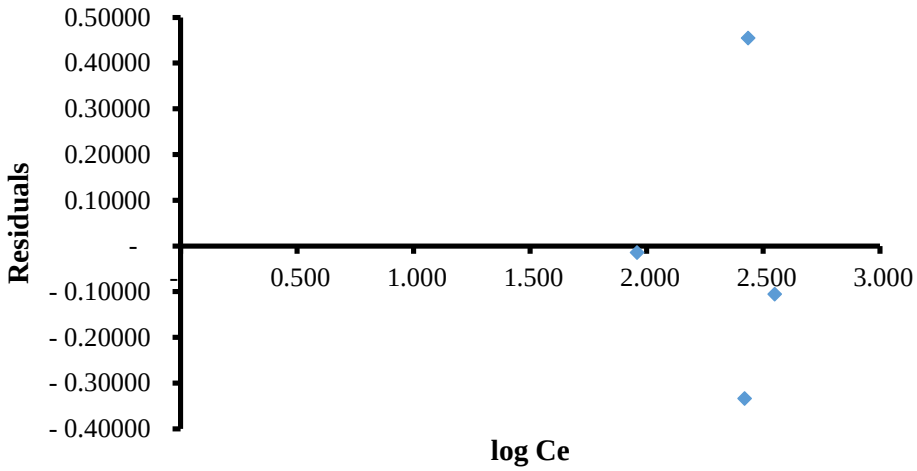


Figure 22: 1/qe and log qe residual plots respectively

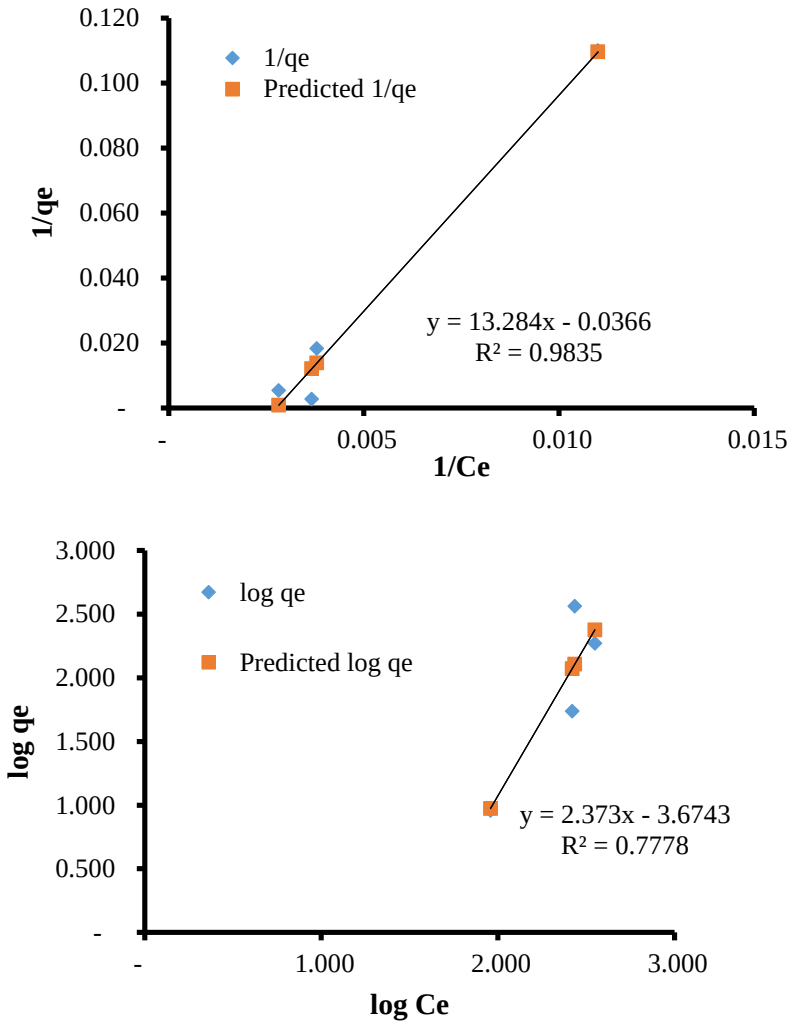


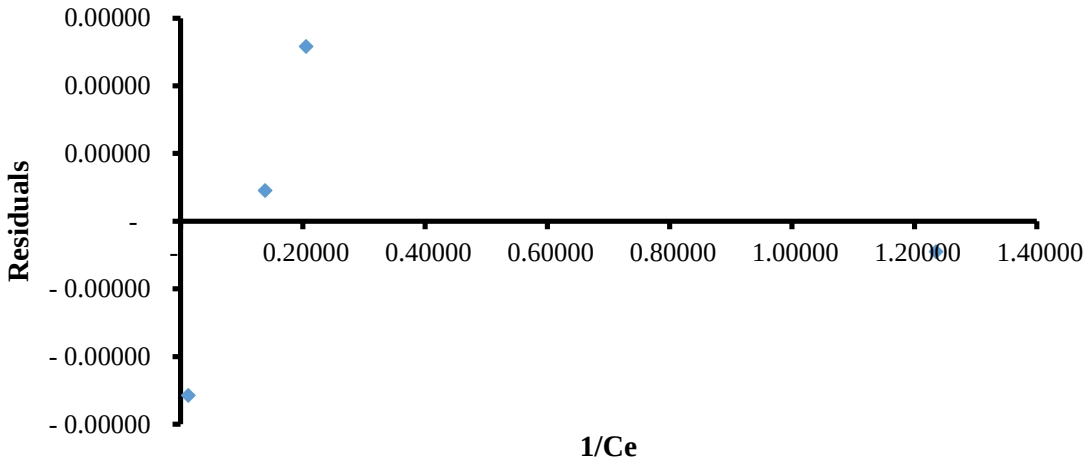
Figure 23: 1/qe and log qe line fit plots respectively

The Langmuir model was favourable, the calculated R_L was 0.04. The Freundlich isotherm adsorption strength constant showed a slight favourability with 1/n of 0.328. The calculated 1/n value is low as compared to that obtained when Chloramine T was used as an adsorbent. This implied that the Freundlich model is more favourable when Chloramine T is used as an adsorbent as compared to with Synthesised PI as an adsorbent.

4.1.2.1.3 Chloramine T as an adsorbent in diesel oil desulphurisation

In the desulphurisation of Diesel fuel 1, the best fit was found to be in the Freundlich model, the attained R square values were 0.435 and 0.881 for Langmuir and Freundlich respectively. The obtained Langmuir RL value was 1 and according to Lam and Ridzuan (2008) this suggested that the Langmuir adsorption was unfavourable. The adsorption strength constant in the Freundlich model was 272.41 which indicated a high favourability.

It was also observed in the residual plot below that the Freundlich fitted better as compared to Langmuir, refer to Figure 21 and 22.



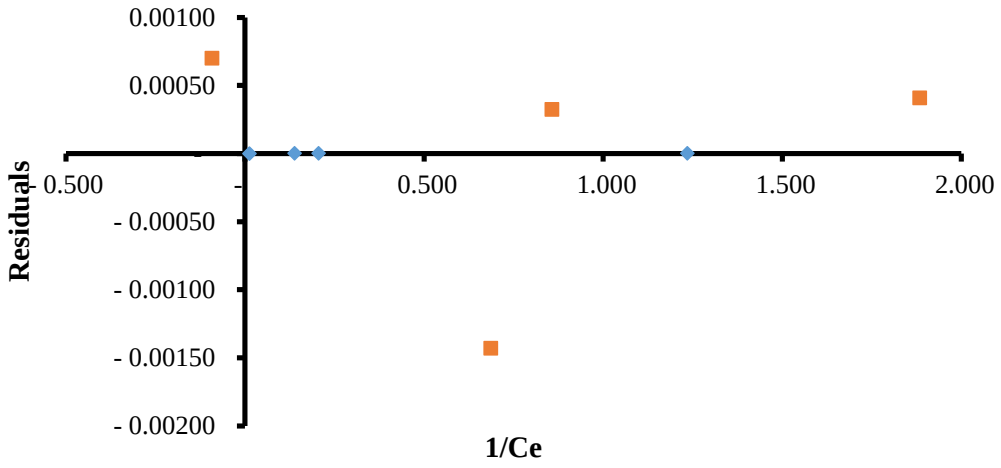


Figure 24: 1/qe and log qe residual plots respectively

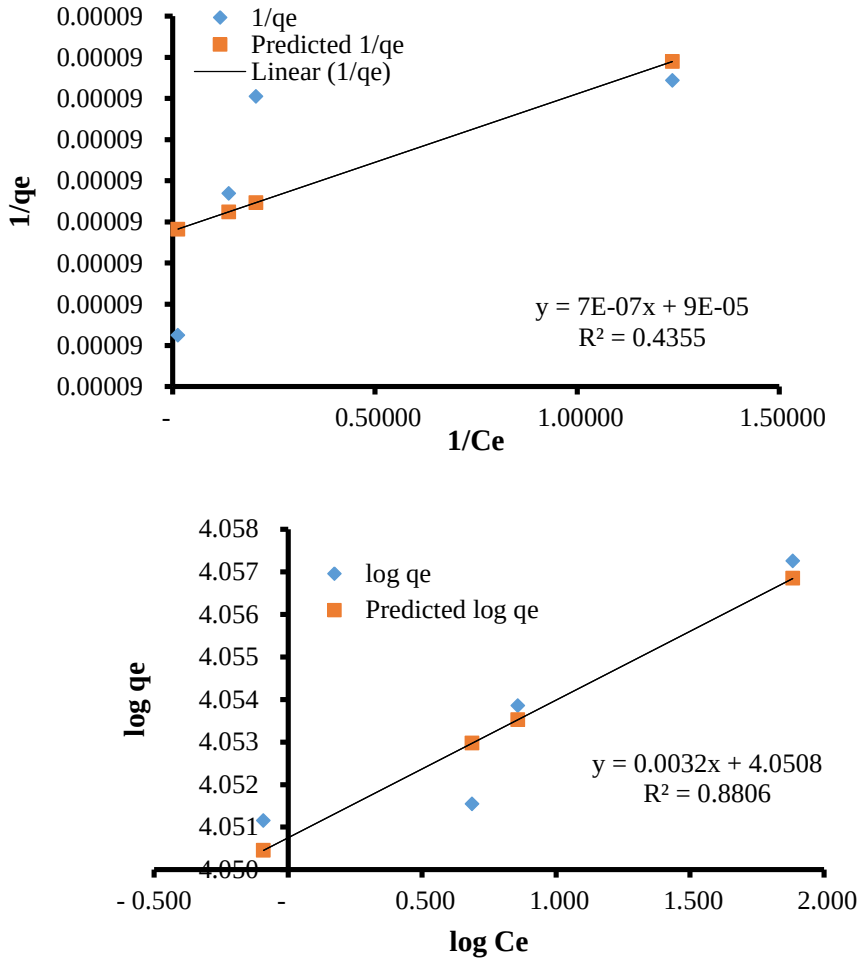


Figure 25: 1/qe and log qe line fit plots respectively

In the desulphurisation of Diesel fuel 2, both models were found to be unfavourable though the Freundlich was found to be slightly favourable as compared to Langmuir (Figure 40 in

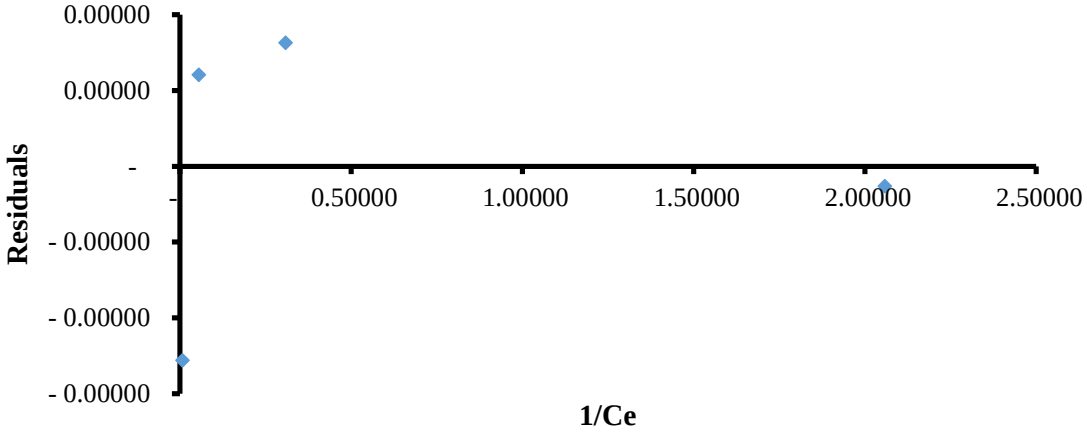
Appendix A.1). The obtained R squared values were 0.218 and 0.433 for Langmuir and Freundlich respectively. The Langmuir separation factor confirmed the in-favourability at 1 and the Freundlich adsorption strength factor was 6.052, which is very low as compared to that of Diesel fuel 1.

The low favourability can be confirmed by the slow desulphurisation rate observed during the experiment and also the low desulphurisation efficiency. According to Fadhel, 2010, the low desulphurisation efficiency in diesel fuel 2 might be due to the DBT's low polarity sulfimides which have large carbon number of substituents that might be formed by reacting with chloramine T.

4.1.2.1.4 Synthesised PI as an adsorbent in diesel oil desulphurisation

The best fit in the Diesel fuel 1 desulphurisation was also found to be in the Freundlich model, the attained R square values were 0.258 and 0.747 for Langmuir and Freundlich respectively. The adsorption strength constant in the Freundlich model was 176.63 which indicated a high favourability.

It was also observed in the residual plot in Figure 26 that the Freundlich was a better fit as compared to the Langmuir model.



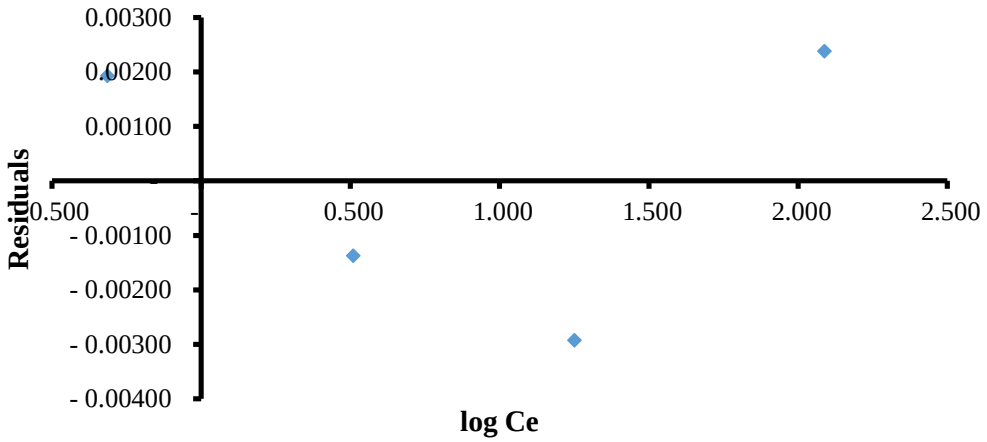


Figure 26: 1/qe and log qe residual plots respectively

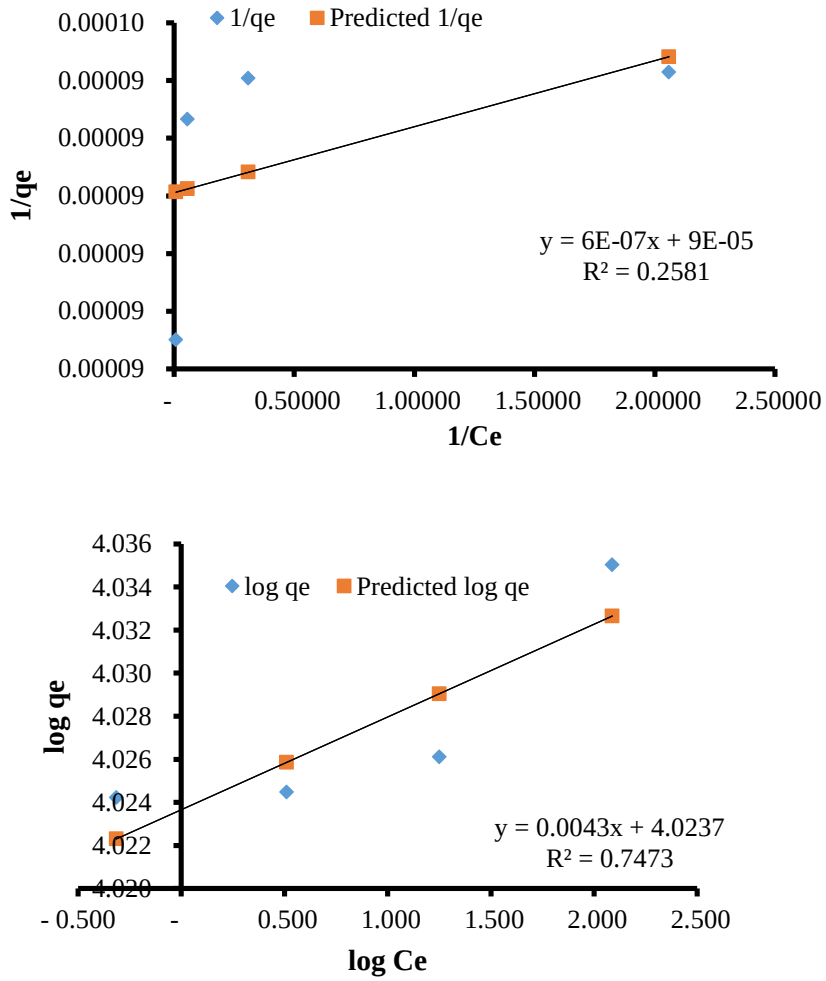


Figure 27: 1/qe and log qe line fit plots respectively

Both Langmuir and Freundlich models were found to be less favourable in the desulphurisation of Diesel fuel 2 (Figure A.2 in Appendix A). The attained R square values

were 0.084 and 0.022 for Langmuir and Freundlich respectively. The Freundlich adsorption strength was low as 2.65 and the Langmuir separation factor confirmed that this model was less favourable, the calculated value was 1.

4.1.2.2 Adsorption Kinetics

4.1.2.2.1 Chloramine T as an adsorbent in model light oil desulphurisation

This adsorption process fitted the pseudo-first order model. The obtained linear regression R squared value was 0.987. The actual ln(qe-qt) versus predicted ln(qe-qt) plot confirmed that the pseudo first order was the best fit, Figure 28. The first-order adsorption equilibrium rate constant was calculated to be 0.018 min^{-1}.

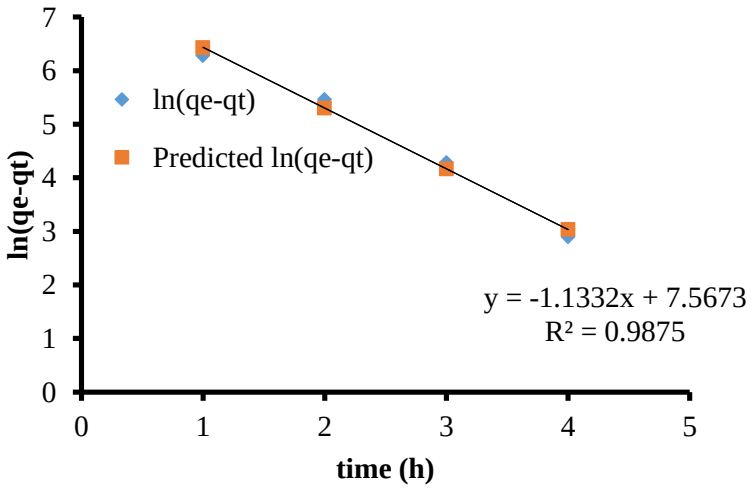


Figure 28: ln(qe qt) line fit plots respectively

4.1.2.2.2 Synthesised PI as an adsorbent in model light oil desulphurisation

This process best fitted the first order model. An R squared value of 0.955 was obtained through linear regression. The actual ln(Ct) versus predicted ln(Ct) plot in Figure 29 confirmed that the first order is the best fit, Figure 29. The first-order adsorption equilibrium rate constant was calculated to be 0.009 min^{-1}.

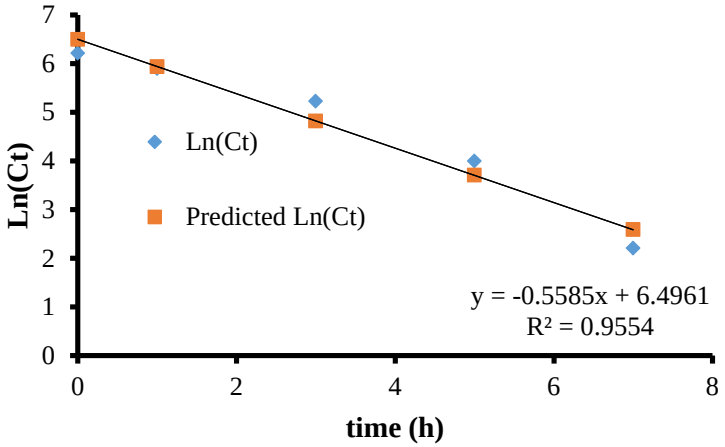


Figure 29: Synthesised PI in Model Light Oil ln(Ct) line fit plots

4.1.2.2.3 Chloramine T as an adsorbent in diesel oil desulphurisation

The Diesel fuel 1 and 2 adsorption process fitted the pseudo second and third order, respectively. The obtained linear regression R squared values were 0.694 and 0.889 for the pseudo second and third order model, respectively. The equilibrium rate constants were also calculated and were $0.02min^{-1}$ and $0.07e^{-8}$ min^{-1} for the pseudo second and third order model.

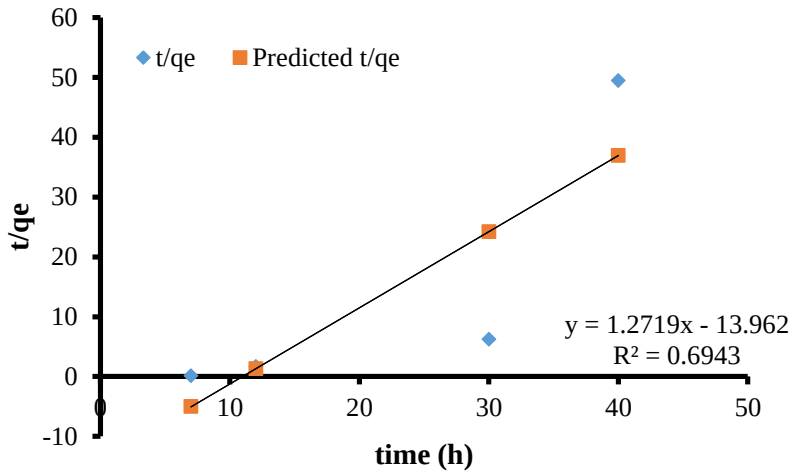


Figure 30: Chloramine T in Diesel fuel 1 ln(t/qe) line fit plots

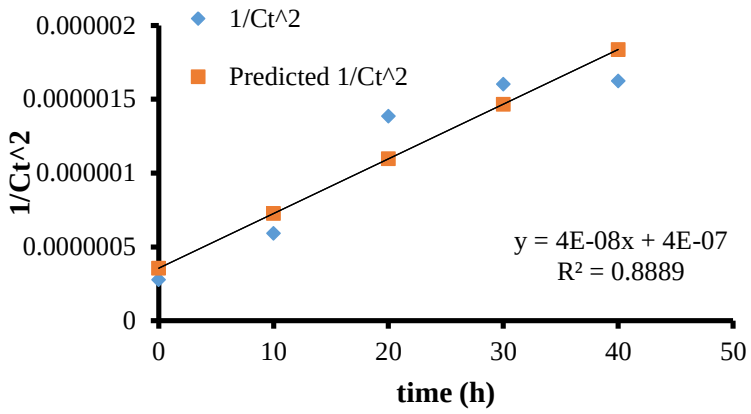


Figure 31: Chloramine T in Diesel fuel 2 $1/C_t^2$ line fit plots

4.1.2.2.4 Synthesised PI as an adsorbent in diesel oil desulphurisation

The Diesel fuel 1 and 2 adsorption process fitted the pseudo-first order and third order model, respectively. The obtained linear regression R squared values were 0.999 in the Diesel fuel 1 and 0.774 in the Diesel fuel 2. The data $\ln(q_e-q_t)$ and $1/C_{t2}$ versus predicted plots confirmed that the pseudo first order was the best fit, refer to Figure 32. The first-order adsorption equilibrium rate constant was calculated to be 0.003 min^{-1} and the third order equilibrium rate is $0.03e^{-8}$ min^{-1}.

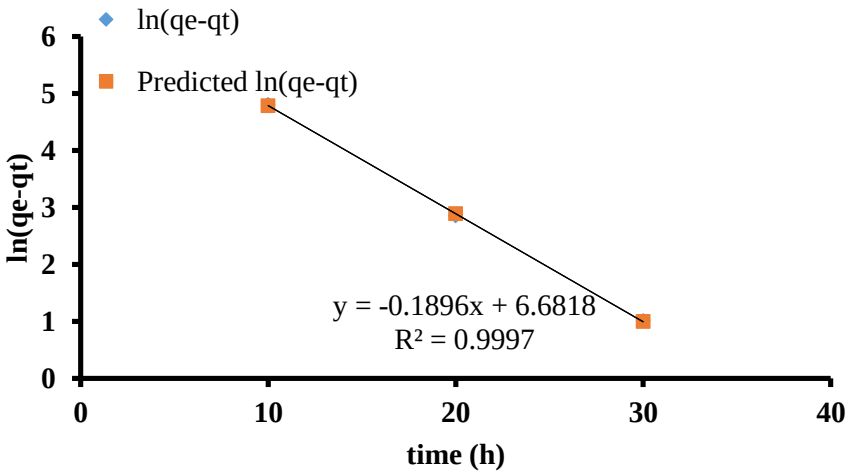


Figure 32: Synthesised PI in Diesel fuel 1 ln(qe-qt) line fit plots respectively

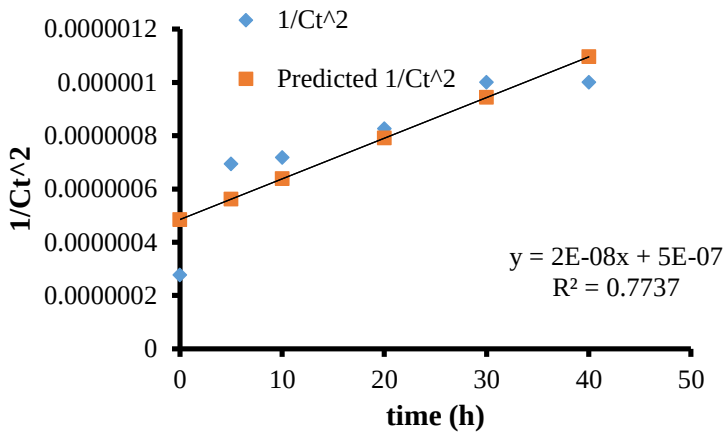


Figure 33: Synthesised PI in Diesel fuel 2 $1/C_t^2$ line fit plots respectively

5 MODEL DEVELOPMENT FOR MASS TRANSFER IN ADSORPTION PACKED BED

5.1 Mathematical Model

The main objective of a mathematical model is to predict the adsorption performance given certain constrains. Modelling proved to be critical in design cases where the purpose is to obtain the packed column specifications such as a) length b) bed cross sectional area c) type and size of the particle and e) the amount of particles and operational conditions. In the development of an adsorption model, three adsorption equations are adopted given certain assumptions and conditions:

1. The mass transfer from liquid phase to solid phase
2. The mass transfer within the particles
3. The adsorption isotherm equation

Operational conditions can be important depending on the resistance to mass and heat transfer, both inside and outside the sorbent pellet. Either can be neglected in favour of the other. Instantaneous rate of adsorption is usually assumed in most models, (Shaverdi, 2012). The models usually assume that the local rate of adsorption is instantaneous compared to transport processes.

The proposed model was derived using the equations below:

1. Mass balance equation for the bulk flow in the bed, neglecting radial dispersion:

$$-D_{ax}\frac{\partial^2 C_{(x,t)}}{\partial x^2} + u\left(\frac{\partial C_{(x,t)}}{\partial x}\right) + C_{(x,t)}\left(\frac{\partial u}{\partial x}\right) + \left(\frac{\partial C_{(x,t)}}{\partial t}\right) + \frac{(1-\varepsilon)}{\varepsilon}\left(\frac{\partial q_T}{\partial t}\right) = 0 \qquad (5\text{-}1)$$

With D_{ax} being an axial dispersion coefficient, C initial sulphur concentration in the fuel, x the axial distance, u the superficial velocity, ε the bed porosity, t the time, and q_T the adsorption capacity. The follow assumptions were made:

- Laminar flow and no axial mixing. Axial mixing through the packed bed reduces the adsorption process efficiency. Ruthven (1984) identified the two mechanisms the causes axial mixing as being Molecular diffusion and turbulent mixing.

$$D_{ax}\left(\frac{\partial^2 C_{(x,t)}}{\partial x^2}\right) = 0 \qquad (5\text{-}2)$$

- The interstitial velocity, *u*, being the fluid velocity inside the bed among the particles and was correlated to the superficial velocity. u was assumed to be constant.

$$C_{(x,t)}\left(\frac{\partial u}{\partial x}\right) = 0 \qquad (5\text{-}3)$$

- The concentration gradients in both the radial and longitudinal direction was assumed to be negligible. For a bed/pellet diameter ratio of greater than 20, channelling at the wall and random variation in the interstitial velocity within the bed was assumed to be negligible, (Shaverdi, 2012).

- An isothermal process was assumed, this implied constant temperature.

- The equilibrium of adsorption was described by the theoretical Langmuir isotherm.

Incorporating the assumption above reduces equation (5-1) to:

$$u\left(\frac{\partial C_{(x,t)}}{\partial x}\right) + \left(\frac{\partial C_{(x,t)}}{\partial t}\right) + \frac{(1-\varepsilon)}{\varepsilon}\left(\frac{\partial q_T}{\partial t}\right) = 0 \qquad (5\text{-}4)$$

$\frac{\partial q_T}{\partial t}$ was defined as the loss due to adsorption and it showed mass transfer from the fluid phase to the solid phase. There were different ways of obtaining the rate of adsorption viz. quasichemical, linear rate-fluid film, linear rate-solid film and solid diffusion models. Based on the developed model, the linear rate-fluid film model was used. The linear rate-fluid film model assumed that the correlation between the sorbed phase concentration for a single particle (q) and the gas phase concentration in the bulk was:

$$\left(\frac{\partial q_T}{\partial t}\right) = h_m * a_p * \left(C_{(x,t)} - C^*\right) \qquad (5\text{-}5)$$

Where, (Shaverdi, 2012):

h_m is the convective mass transfer coefficient [m/s]

a_p is the external surface area per particle unit volume [m^2/m^3]

C^* is the fluid phase concentration in the laminar flow adjacent to each particle [mg/m^3]

According to Yusuf et al. (2013) *C** is in equilibrium with the sorbed phase concentration at the surface of the adsorbent particle Qs. When the particle total adsorption rate is obtained the available adsorption surface area should always be considered. The adsorption equation was described by Langmuir Isotherm:

$$Q_s = \frac{Q_m b C^*}{1+bC^*} \tag{5-6}$$

Rearranging equation (5-6) gives:

$$C^* = \frac{Q_s}{Q_m - Q_s b} \tag{5-7}$$

Putting equation 5-7 into equation 5-5 gives:

$$\left(\frac{\partial q_T}{\partial t}\right) = h_m * a_p * \left(C_{(x,t)} - \frac{Q_s}{(Q_m b - Q_s b)}\right) \tag{5-8}$$

Putting equation 5-8 into equation 5-4 gives:

$$u\left(\frac{\partial C_{(x,t)}}{\partial x}\right) + \left(\frac{\partial C_{(x,t)}}{\partial t}\right) + \frac{(1-\varepsilon)}{\varepsilon}\left(h_m * a_p * \left(C_{(x,t)} - \frac{Q_s}{(Q_m b - Q_s b)}\right)\right) = 0 \tag{5-9}$$

The following initial conditions were considered:

$C_{(0,t)} = C_0$, $\frac{\partial C(L,t)}{\partial x} = 0$ for t>0 where C_0 is the initial concentration

$C_{(x,0)} = 0$ 0<x<L

5.2 Comparison against other models

The developed model was compared against, Babu (2005) and Yusuf et al. (2013)'s models. The differences are detailed in the table below.

Table 14: Model comparison

	Babu, 2005	Yusuf et al. (2013)	Developed Model
The system operates under Isothermal conditions	Yes	Yes	Yes
There is a non-linear adsorption equilibrium relationship described by Langmuir isotherm	Yes	Yes	Yes
The velocity amongst the bed particles varies along the column	Yes	Yes	No
The velocity amongst the bed particles is constant throughout the column	No	Yes	Yes
The flow pattern in the bed can be described by an axial dispersion plug flow	Yes	Yes	No
The flow pattern is laminar and there is neither axial mixing nor dispersion.	No	No	Yes
The inter-phase transfer rate is expressed by:	$\left(\frac{\partial q_T}{\partial t}\right) = \frac{3k_f}{\rho_s a_p}(c_b - c_s)$	$\left(\frac{\partial q_T}{\partial t}\right) = \frac{3k_f(1-\varepsilon_p)}{l_p a_p}(c_b - c_s)$	$\left(\frac{\partial q_T}{\partial t}\right) = h_m * a_p * (c_b - c_s)$, (Shaverdi, 2012)

5.3 Simulation Technique

The proposed model was executed with Microsoft Excel Visual Basic. The partial differentials were reduced to linear equations through the explicit Euler's numerical method. The mass balance for all the sections were solved consecutively during the bed residence time. This process was repeated for the next steps until all sections were saturated.

To solve for the differential equation numerically the derivatives in the equation (5-9) were replaced with finite difference approximations on a discretized domain:

$$u\frac{dC_{(x,t)}}{dx} = u\frac{C_{(x+\Delta x,t)} - C_{(x,t)}}{\Delta x} \tag{5-10}$$

Where, Δx is the length of each bed section:

$$\Delta x = \frac{L}{N} \tag{5-11}$$

Where, L is the length of the bed, and N is the number of bed sections. Sections of the bed were assumed to be of equal size.

$$\frac{dC_{(x,t)}}{dt} = \frac{C_{(x,t+\Delta t)} - C_{(x,t)}}{\Delta t} \tag{5-12}$$

Where, Δt is the sections residence time.

$$\Delta t = \frac{t_R}{N} \tag{5-13}$$

Where t_R is the bed residence time

$$t_R = \frac{L}{u} \tag{5-14}$$

If:

$a = u\frac{\Delta t}{\Delta x}$ and

$b = \Delta t * h_m * a_p * \left(\frac{1-\varepsilon}{\varepsilon}\right)$

Therefore:

$$C_{(x,t+\Delta t)} = a * \left(C_{(x,t)} - C_{(x+\Delta x,t)}\right) + (1-b) * C_{(x,t)} + b * C^* \tag{5-15}$$

5.4 Simulation Parameters

The Model parameters, Synthesis PI properties and the equilibrium parameters are listed below.

Table 15: Simulation model parameters

Parameter	Symbol	Value	Unit
Bed porosity	e	0.58	m^2 / s
Maximum adsorption capacity	Q_m	45.4	mg / g
Saturated adsorption capacity	Q_s	27.2	mg / g
Langmuir Isotherm constant	b	0.84	ml / mg
Initial Concentration	C_0	1.9	mg / l
Convective mass transfer coefficient	h_m	0.70	m / s
Superficial velocity	u	0.1	m / s
External surface area per volume of bed	a_p	0.95	m^2 / m^3
Bed length	*L*	0.284	M

The simulation parameters were taken from Babu (2005) and Yusuf et al. (2013) adsorption column specification.

5.5 Simulation Results

5.5.1.1 Simulation breakthrough curve

The breakthrough curve simulation plotted in Figure 34, is similar to that obtained and described in literature by Shaverdi (2012), Babu (2005) and Yusuf et al. (2013).

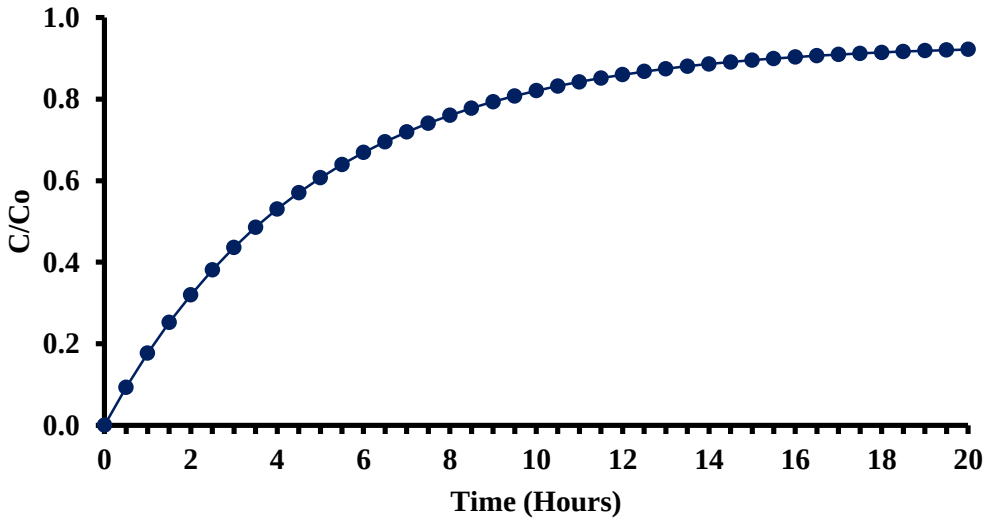


Figure 34: Desulphurisation through adsorption breakthrough curve

The simulation run was 20 hours with an initial concentration of Fadhel (2010)'s diesel fuel 2 of 1900 ppm. The point at which the concentration spikes as the unabsorbed concentration commence to emerge is referred to as the break point, Shaverdi, 2012. The simulation breakpoint was achieved. At C/C_0 of 0.9 and ~10 hours the bed became ineffective (i.e. equilibrium was reached and no adsorption was taking place). The effluent concentration will not be zero if the MTZ length is longer than that of the adsorbent bed. According to Shaverdi (2012) the MTZ is not instantaneous and it is formed over time.

The effect of initial concentration, adsorbent particle size and bed porosity was analysed. The studied parameter was varied while keeping the other parameters constant. The resulting findings are discussed below.

5.5.1.2 Effect of initial concentration on simulated breakthrough curve

The initial adsorbate concentration effect on breakthrough curve is shown in Figure 35. For larger feed concentrations the breakthrough curve steepness decreased thus the breakthrough time increased with an increase in initial adsorbate concentration. The isotherm gradient was lower at higher concentrations which resulted in a higher driving force along the adsorbent bed pores. Also at higher feed concentration, the mass transfer flux was lower from bulk solution to the particle because of the weaker driving force.

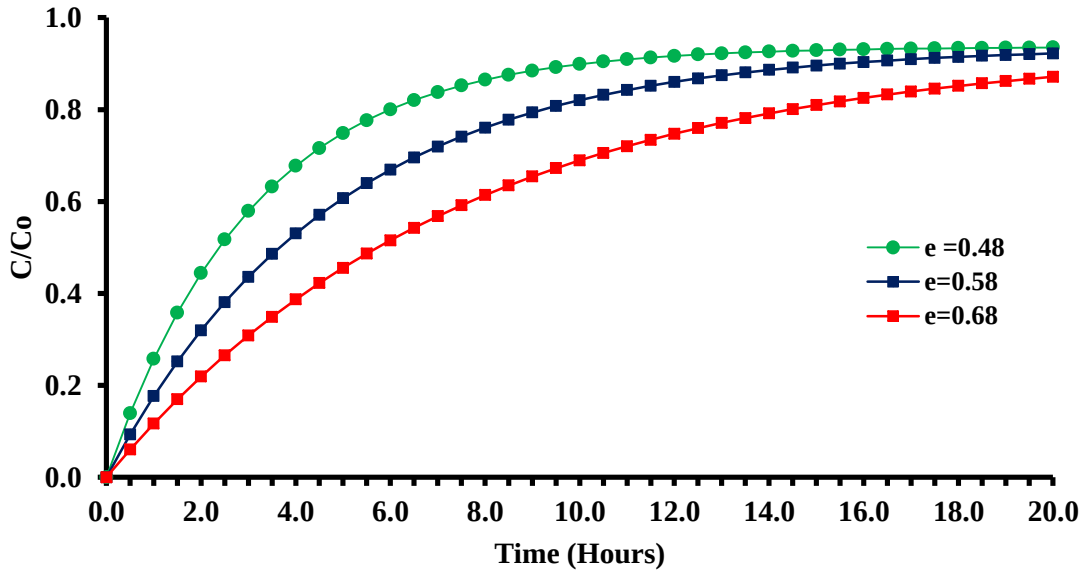


Figure 35: Bed porosity effect on simulated breakthrough curve

5.5.1.3 Effect of external surface area per bed volume on simulated breakthrough curve

It was observed in Figure 36 that as the particle radius increased the breakthrough curve steepness decreased. According to Yusuf et al. (2013) as the particle diameter increased the stagnant film surrounding the particle also increased, resulting in an increase in the time taken by the adsorbate to reach the adsorbent active sites (i.e. the diffusional path was longer). Subsequently the overall process kinetics was slow.

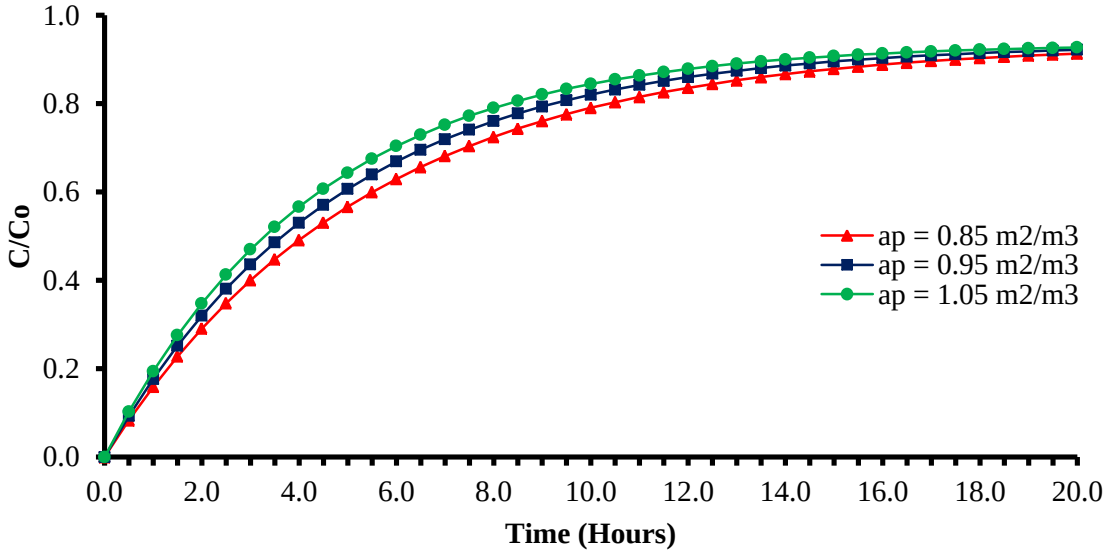


Figure 36: External surface area per bed volume effect on simulated breakthrough curve

5.5.1.4 Effect of bed porosity on simulated breakthrough curve

An increase in bed porosity was observed to reduce the breakthrough curve steepness. This implied that bigger bed porosity reduced the adsorption rate hence lower performances. The smaller bed porosity increased the adsorption rate by reducing the required solute residence time.

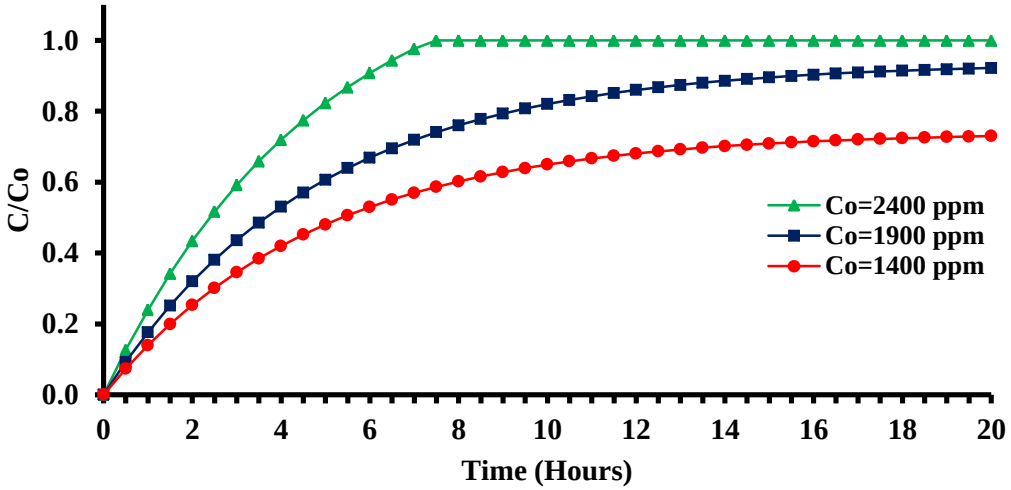


Figure 37: Effect of bed porosity on simulated breakthrough curve

5.6 Simulation model Validation

The developed model was validated against Fadhel (2010) experinmental data to examine its accuracy in predicting the adsorption process.

5.6.1 Breakthrough curve

The experiment and simulation breakthrough curves in Figure 38 were comparable. At time 0 hours when adsorption has not taken place the dimensionless concentration was zero in both the simulation and experiment. As the process progresses, there was an initial exponential increase in C/C_0 as the sulphur breaks through the adsorbent bed and levels off as the adsorption bed become exhausted or inactive. However there was a slight difference in the simulation as compared to the experiment, this was due to the assumptions used to simplify

the model such as isothermal conditions, laminar flow characteristics and constant velocity along the column and this might vary in reality and during experimental conditions.

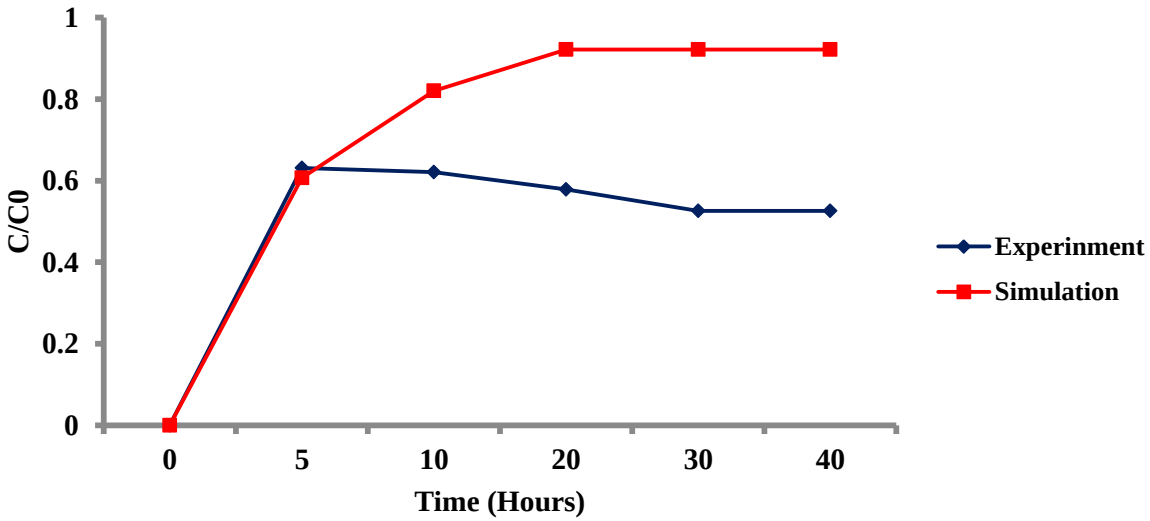


Figure 38: Simulation versus Experiment breakthrough curve

5.6.1.1 Effect of initial concentration

Figure 39 indicated that the simulation was in agreement with the Fadhel (2010)'s experimental data. For larger feed concentrations the breakthrough curve steepness decreased, similarly in the simulation prediction in section *5.6.1*. Thus the model can be used to predict an adsorption process.

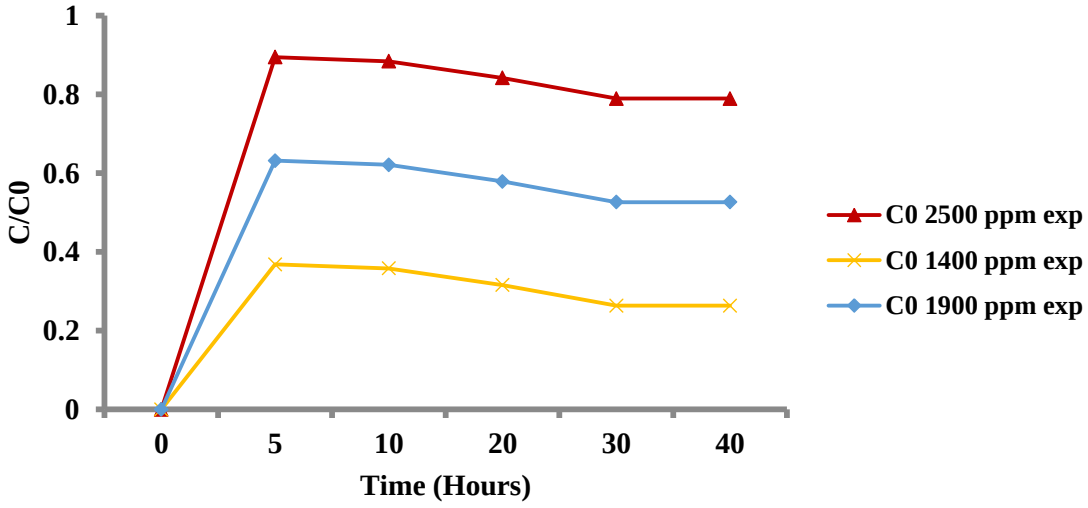


Figure 39: Simulation versus Experiment breakthrough curve

6 CONCLUSION

Fadhel (2010) conducted two sets of adsorption experiments in which the objective was to investigate if adsorbents Chloramine T and Synthesis PI can deep desulphurise light oil and refinery diesel. In the first experiment light oil was modelled using N-tetradecane solution containing 11 mmol/l of DBT and in the second refinery diesel1 from Al-Dura refinery and diesel fuel 2 from Beji refinery were used whilst keeping the adsorbent and experimental conditions the same. The sulphur content in the modelled light oil, diesel fuel 1 and diesel fuel 2 were 500ppm, 12354ppm and 1900ppm respectively.

The experimental findings showed that modelled light oil can be desulphurise to the Euro 5 level requirements, Sulphur <500ppm, by both Chloramine T and Synthesis PI. A complete sulphur removal was achieved using both adsorbents however the desulphurisation rate was faster with Chloramine T as an adsorbent as compared to when Synthesis PI was used.

The adsorption of modelled light oil was found to obey the pseudo-first-order kinetics and the overall adsorption rate was controlled by the chemisorption process. It was observed that the modelled light oil fitted Langmuir isotherm the best, regardless of the adsorbent used. According to Castellan (1983) Langmuir isotherm best describe a chemisorption process. In a chemisorption adsorption process only a monolayer adsorption is feasible as this process involves a more specific binding of the adsorbate onto the solid. Thus it might be concluded that in the desulphurisation of modelled light oil, which is lightly concentrated with Sulphur (initial concentration ≤500ppm), the adsorbent surface is in contact with an adsorbate solution which is strongly attracted to the surface. In this case adsorbent regeneration might be a challenge.

Both Diesel fuel 1 and Diesel fuel 2 could not be desulphurised to the Euro 5 level. The Diesel fuel 1 sulphur concentration was reduced from 12 354 to ~11 200ppm and diesel fuel 2 from 1 900 to 800ppm. It was observed that the rate of desulphurisation proved to be faster with Diesel fuel 1 with a higher initial concentration of 12 354ppm as compared to that of diesel fuel 2 with an initial sulphur content of 1900ppm.

The Freundlich isotherm was found to be a best fit in the adsorption of diesel fuel 1 meaning that the adsorption rate was controlled by a physisorption process where the adsorbate is

bonded onto the solid through the week van der Waals interaction. In this type of adsorption a multi-layered reaction is possible but the process can be easily disrupted by an increase in temperature, thus adsorbent regeneration is feasible. The Diesel fuel 2 desulphurisation process did not fit the studied adsorption isotherms. This was unexpected as the achieved sulphur removal efficiency was 90.63% compared to that of 14.35% of Diesel fuel 1. It was expected that the Langmuir will be a best fit since high sulphur removal efficiency indicate a stronger relationship between adsorbent and adsorbate.

Diesel fuel 1 adsorption reaction obeyed the pseudo-second and pseudo-first order kinetics when reacted with Chloramine T and Synthesis PI, respectively. The obtained R squared values were 0.694 and 0.999 for pseudo-second and pseudo-first order, respectively. Diesel fuel 2 obeyed the third order kinetics with both Chloramine T and Synthesis PI, with R squared values calculated at 0.889 and 0.774 for Chloramine T and Synthesis PI reaction, respectively.

The adsorption kinetics and isotherm findings on diesel fuel 1 are supported by the studies conducted by Muzic, et al. (2008) and Nazal, et al. (2015). In these studies it was found that the adsorption process favours the pseudo-second order kinetics and can be best described by the Freundlich isotherms model.

A mathematical model for a fixed bed was developed and solved numerically by implicit forward Euler finite difference method. The model was then simulated using Microsoft Excel Visual Basic, which is a programming function on Excel. The simulation findings showed that the adsorbate residence time reduced by smaller adsorbent bed porosity resulting in increased adsorption rate. By decreasing the adsorbent particle diameter and increasing the initial sulphur concentration, the breakthrough time is decreased.

When validated against the experimental data, the experiment data agreed with the simulation results. This confirmed that the proposed model is applicable to study the performance of fixed bed adsorption processes under isothermal conditions, no axial mixing and constant interstitial velocities.

7 RECOMMENDATIONS

The obtained results can assist in improving modelling of adsorption processes especially during adsorption column design. To improve on the developed model, future studied can include:

- Testing in non-isothermal systems where axial dispersion or mixing is not negligible.
- Take into account effluent stream recycle and adsorbent bed regeneration.
- To reduce capital and operation cost in commercial plant, investigate agencies that will improve adsorption rates.

Also to ensure accuracy in the developed model, model validation on the bed porosity and external surface area per particle volume should be investigated further.

8 BIBLIOGRAPHY

Agarwal, P. & Sharma, D. K., 2010. Comparative studies on the biodesulfurization of crude oil with other desulfurization techniques and deep desulfurization integrated processes. *Energy Fuels,* Volume 24, pp. 518-524.

Anon., 2002. Desulfurization. *Hydrocarbon Engineering,* 7(7), pp. 25-28.

Babich, I. V. & Moulijn, J. A., 2003. Science and technology of novel proceesses for deep desulfurization of oil refinery streams. *Fuel,* pp. 82:607-631.

Bavu, B. V. & Gupta, S., 2005. Modelling and simulation of fixed bed adsoprtion column: effect of velocity variation. *J. Eng. Technol,* Volume 1, pp. 60-66.

Brieva, G. B., Campos-Martin, J. M., Al-Zahrani, S. M. & Fierro, J. L., 2010. Removal of refractory organic sulphur compounds in fossil fuels using MOF sorbeents. *Glob NEST J,* pp. 12:296-304.

Castellan, G. W., 1983. *Physical Chemistry.* third ed. New York: Addison-Wesley.

Darwish, N. N., 2015. *Adsorption study of desulfurization of diesel oil using activated charcoal,* Sharjah, United Arab Emirates: American University of Sharjah.

Fadhel, Z. S., 2010. *Desulfurization of light diesel fuel using chloramine T and Polymer supported imidation agent,* s.l.: Ministry of higher education & scientific reserch university of technology chemical engineering department.

Fei, L. et al., 2017. Equilibrium and kinetic studies on the adsorption of thiophene and benzothiophene onto NiCeY zeolites. *The Royal Society of Chemistry,* Issue 7, pp. 23011-23020.

Freundlich, U., 1906. The Adsorption Solution. pp. 385-470.

Gary, J. H. & Handwerk, G. E., 1984. *Petroleum Refining Technology and Economics.* 2nd ed. s.l.:Marcel Dekker, Inc..

Goud, V. V., Mohanty, K., Rao, S. S. & Jayakumar, N. S., 2005. Prediction of mass transfer coefficients in packed bed using tamarind nut shell activated carbon to rmeove phenol. *Chem. Eng. technol,* 28(9), pp. 991-997.

Greenwood, J. M., Johnson, J. S. & Witham, M. J., 2000. *Preparation of Polyethersulfone membranes.* United States of America, Patent No. 6,056,903.

Hamad, F. et al., 2011. *Membrane desulphurisation of liquid hydrocarbons using an extractive liquid membrane contactor system and method.* United States of America, Patent No. 2011/0000823.

Ho, Y.-S., 2006. adsorbate residence time and the reactor dimensions controlled by the system's kinetics (Ho et al., 2006). *Journal of Hazardous Materials,* B(136), p. 681–689.

Ho, Y., 2006. Review of second-order models for adsorption systems. *Journal of Hazardous Materials,* Volume B136, p. 681–689.

Ho, Y. & McKay, G., 1999. Pseudo-second order model for sorption processes. *Process Biochemistry,* Volume 34, p. 451–465.

Irvine, R. L., Benson, B. A. & Varreveto, D. M., 1999. Process low cost breakthrough for low sulphur gasolinee. *NPRA 1999 Annual Meeting,* pp. 99-42.

Jaroniec, M., 1975. Adsorption on heterogeneous surfaces: the exponential equation for the overall adsorption isotherm. *Surface Science,* Volume 50.2, pp. 553-564.

Javadli, R. & de Klerk, A., 2012. Desulfurization of heavy oil. *Appl Petrochem Res,* Volume DOI 10.11007/s13203-0112-0006-6, pp. 1:3-19.

Laboratories, S., 2008. *setlaboratories.* [Online]
Available at: http://www.setlaboratories.com
[Accessed 18 July 2015].

Lam, M. & Ridzuan, Z., 2008.. Production of activated carbon from sawdust using fluidized bed reactor. *International Conference on Environment,.*

Masel, R., 1996. Principles of Adsorption and Reaction on Solid Surfaces. *Wiley Interscience,* Volume ISBN 0-471-30392-5., p. 240.

Mehran, S., Amarjeet, B. & Argyrios, M., 2007. Biodesulfurization of refractory organic sulphur compounds in fossil fuels. *Bitechnol Adv,* Volume 25, pp. 570-596.

Minitab, n.d. *Minitab 17.* [Online]
Available at: http://support.minitab.com
[Accessed 14 June 2016].

Mittal, A., Kurup, L. & Mittal , J., 2006. Kinetics for the Removal of Tartrazine from Aqueous Solutions Using Hen Feathers. *Journal of Hazardous Materials,* Volume 146, pp. 243-248.

Muzic, M. & Sertic-Bionda, K., 2013. Alternative Processes fo rRemoving Organic Sulfu rCompounds from Petroleum Fractions. *Chemical& Biochemical Engineering Quartely,* 27(1), pp. 101-108.

Muzic, M., Sertic-Bionda, K. & Gomzi, Z., 2008. Kinetic and Statistical Studies of Adsorptive Desulfurization of Diesel Fuel on Commercial Activated Carbons. *Chem. Eng. Technol.,* 31(No. 3), pp. 355-364.

Nazal, M. K. et al., 2015. The nature and kinetics of teh adsorption of dibenzothiophene in model diesel fuel on carbonaceous materials loaded with aluminum oxide particles. *Arabian Journal of Chemistry,* pp. 1878-5352.

Okeola, F. & Odebunmi, E., 2010. Adsorption of Methylene Blue by Activated Carbon Derived from Agrowastes. *Advances in Natural and Applied Sciences,* 4(3), pp. 281-288.

Raghavan, N. S. & Ruthven, D. M., 1983. Numerical Simulation of a fixed bed adsorption column by the method of crthogonal Collocatio.. *AICHE,* 29(6), p. 922.

Ramraj, S. & Anandaraj, C., 2014. Removal of sulphur in petroleum refining using DCS. *IOSR Journal of Engineering (IOSRJEN),* 04(05), pp. 19-22.

Sakanishi, F. et al., 2003. Adsorptive removal of sulfur compounds from naphtha fractions by using carbon adsorbents. *American Chemical Society, Division of Fuel Chemistry,* 48(2), p. 524.

Salem, A., 1994. Naphtha desulfuriization by adsorption. *Ind Eng Chem Res,* pp. 33:336-340.

Salem, A., 1997. Removal of sulphur compounds from naptha solutions using solid adsorbents. *Chem Eng Technolgy,* pp. 20:342-347.

Shaverdi, G., 2012. *Developing a model for mass transfer in adsorption packed bed filters,* Montreal, Quebec, Canada: s.n.

Sigma-Aldrich, 2015. *sigma aldrich.* [Online]
Available at: http://www.sigmaaldrich.com
[Accessed 27 July 2015].

Suresh, G. & Bavu, B. V., 2010. *Modelling and Simulation of Fixed Bed Adsorption Column: Effect of operating Variables,* s.l.: s.n.

Thajeel, A. S., 2013. Isotherm, Kinetic and Thermodynamic of Adsorption of heavy metal ions onto local activated carbon. *Aquatic Science and technology,* Vol1(No.2), pp. ISSN 2168-9148.

Wakao, N. & Weatherly , L. R., 1978. Effect of fluid dispersion coefficients on particle fluid mass transfer coefficient in packed beds. *Chemical engineering Science,* Volume 33, pp. 1375-1384.

Yasuhiro, S., Takayuki, H. & Isao, K., 2002. Oxidative Desulfurization Process for Light Oil Using Titanium Silicate Molecular Sieve Catalysts. *Chemical engineering of Japan,* 35(12), pp. 1305-1311.

Yussuff, A. S. et al., 2013. Mathematical modelling of fixed bed adsorption column for liquid. Phase Solute: Effect of Operating variables. *International Journal of Scientific&Engineering Research,* 4(8), pp. 2229-5518.

9 APPENDICES

9.1 APPENDIX A: Langmuir and Freundlich plots for the desulphurization of diesel fuel 2

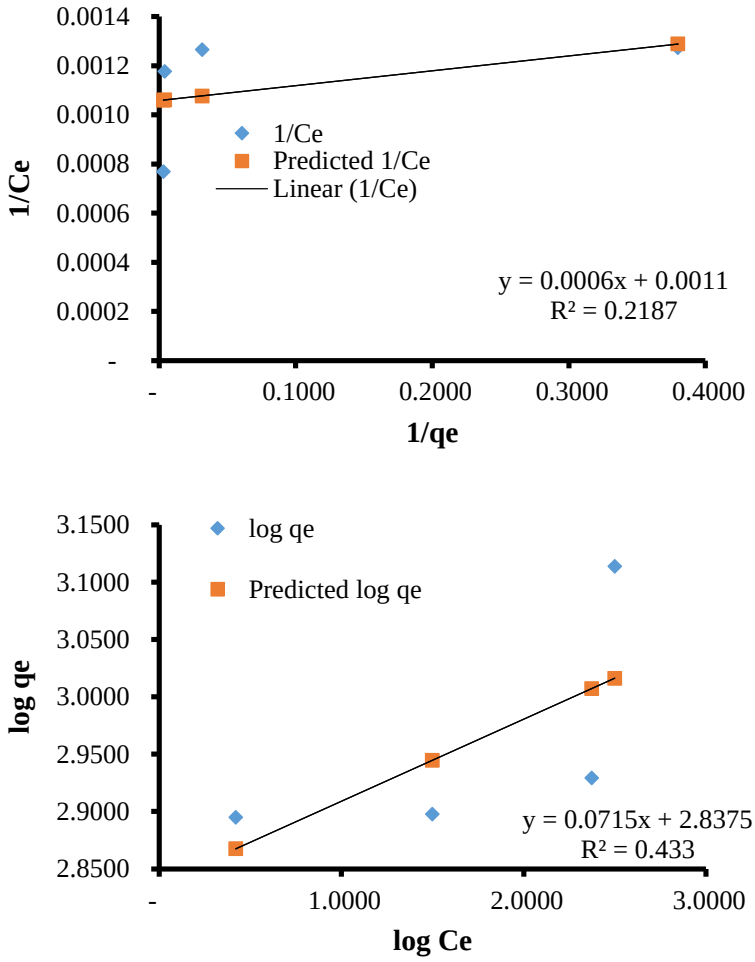
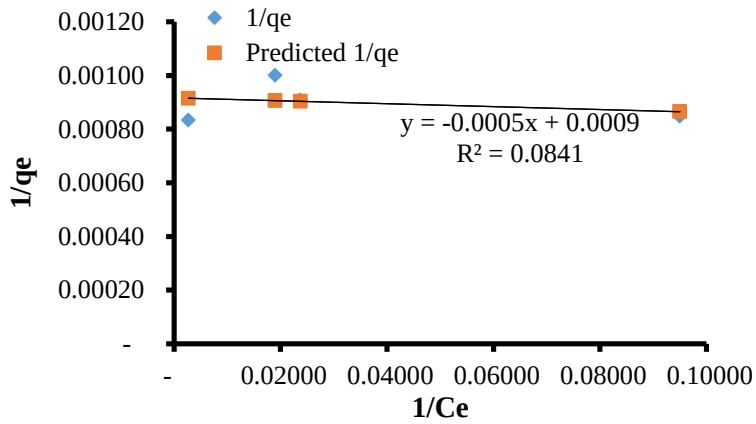


Figure 40: Langmuir and Freundlich plots for Chloramine T as adsorbent of diesel fuel 2



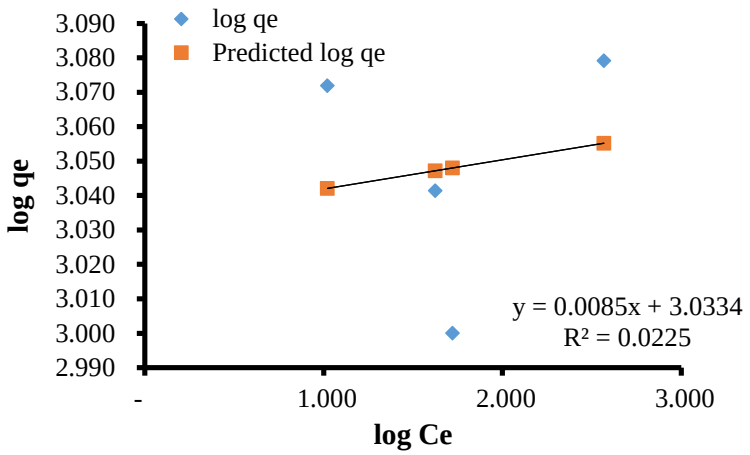


Figure 41: Langmuir and Freundlich plots for synthesized PI as adsorbent of diesel fuel 2

1.2 APPENDIX B: Microsoft Excel Visual Basic Code for Breakthrough Curve

```
Sub Desulph()
'This proceture computes concentration (Cx,t)
    Application.ScreenUpdating = False

' Declaring reference sheet
    Dim shData As Worksheet, shOut As Worksheet, rngS As Range, rngI As Range
    Set shData = Sheets("Data")
    Set shOut = Sheets("Output")
    Set rngS = shOut.Range("A1:A10000")
    Set rngI = shOut.Range("B1:B10000")

'Variables declaration for advection equation
    Dim Lmax, Tmax, e, Qm, Qs, b, Co, hm, u, ap, N, h, dt, dx, Ce

 'Assigning values to variables
    Lmax = shData.Cells(13, 5).Value
    Tmax = shData.Cells(15, 5).Value
    e = shData.Cells(5, 5).Value
    Qm = shData.Cells(6, 5).Value
    Qs = shData.Cells(7, 5).Value
    b = shData.Cells(8, 5).Value
    Co = shData.Cells(9, 5).Value
    hm = shData.Cells(10, 5).Value
    u = shData.Cells(11, 5).Value
    ap = shData.Cells(12, 5).Value
    N = shData.Cells(16, 5).Value
    h = shData.Cells(17, 5).Value

  'Calculating variables
```

```
    Ce = Qs / (Qm * b - Qs * b)
    dt = Tmax / N
    dx = Lmax / N
    alpha = (u * dt / dx) + 1
    beta = dt * ((1 - e) / e) * hm * ap

'Inital value of the function
    Dim i As Integer, k As Integer, lngR As Integer, C, z
        lngR = 2
    'At: t=0 for x>0
    For i = 1 To h + 1
        C = "C(" & i & ",1)"
        shOut.Cells(lngR, 1).Value = C
        C = 0
        shOut.Cells(lngR, 2).Value = C
        z = (1 - 1) * dx
        lngR = lngR + 1
    Next i

    'At: t=1 for x > 0
    For k = 1 To N + 1
        C = "C(1," & k & ")"
        shOut.Cells(lngR, 1).Value = C
        C = 0
        shOut.Cells(lngR, 2).Value = C
        lngR = lngR + 1
    Next k

    'At: x=2 for t > 1
    Dim C2i_1, C3i_1, t, x
    For t = 1 To N
```

```
        For x = 2 To h
            C = "C(" & x & "," & t + 1 & ")"
            shOut.Cells(lngR, 1).Value = C
            C2i_1 = "C(" & x & "," & t & ")"
            C2i_1 = Application.WorksheetFunction.Match(C2i_1, rngS, 0)
            C2i_1 = Application.WorksheetFunction.Index(rngI, C2i_1)
            C = (1 - (beta / alpha)) * C2i_1 + (beta / alpha) * Ce
            shOut.Cells(lngR, 2).Value = C
            lngR = lngR + 1
        Next x
    Next t
    Application.ScreenUpdating = False
End Sub
```